LECTURE WB3413/OE4626 DREDGING PROCESSES

CUTTING OF ROCK
(January 2007)

Prof. ir. W.J. Vlasblom

CONTENTS

Introduction

Rock is a natural occurrence mass of cohesive organic or inorganic material, which forms a part earth crest of which most rocks are composed of one or more minerals. [van Rossen, 1987]

Rocks can be classified in different ways. The most used classification is based on their origin, in which the following classes can be distinguished.

1. Igneous rock; a rock that has solidified from molten rock material (magma), which was generated within the Earth. Well known are granite and basalt
2. Sedimentary rock; a rock formed by the consolidation of sediment settle out in water, ice of air and accumulated on the Earth's surface, either on dry land or under water. Examples are sandstone, lime stone and clay stone
3. Metamorphic rock; any class of rocks that are the result of partial or complete recrystallisation in the solid state of pre-existing rocks under conditions of temperature and pressure that are significantly different from those obtaining at the surface of the Earth.

Table 1

Table A1 Aid to identification of rock for engineering purposes (after BS 5930:1981).

GRAIN SIZE (mm)	Bedded rocks SEDIMENTARY						Foliated rocks METAMORPHIC	Massive and crystalline rocks IGNEOUS				GRAIN SIZE (mm)
Coarse	RUDACEOUS: CONGLOMERATE (rounded particles in a finer matrix); BRECCIA (angular particles in a finer matrix)	rocks with mixed composition (Clark and Walker 1977)**	calcirudite	CLASTIC LIMESTONE: conglomerate limestone	CRYSTALLINE LIMESTONE & Dolomite	EVAPORITES: Halite, gypsum, anhydrite	GNEISS (Sometimes massive): Well developed but often widely spaced foliation sometimes with schistose bands	GRANITE (1,2)	DIORITE (1,2)	GABBRO (1,3)	PERIDOTITE	Coarse
2							MIGMATITE: mixture of gneiss and veins of igneous rock					2
0.6 – Medium 0.2 – 0.06	ARENACEOUS: SANDSTONES (Quartz) ARENITE: Quartz grains and siliceous cement; (Quartz) ARKOSE: Many feldspar grains usually with some mica; (Quartz)(grey) WACKE: Many rock chips; TUFF (CEMENTED VOLCANIC ASH)		calcarenite	detrital limestone			SCHIST: Well developed foliation generally much mica; METAMORPHOSED LIMESTONE (Marble); SERPENTINITE; AMPHIBOLITE; QUARTZITE	MICRO-GRANITE (1,2) (Porphyry)*	MICRO-DIORITE (1,2) (Porphyry)*	DOLERITE (3) (Porphyry)*		Medium 0.06
Fine 0.002	ARGILLACEOUS: SILTSTONE: Mostly silt; CLAYSTONE: Mostly clay (massive texture); SHALE (fissile texture)		calcilutite calcisiltite	fine grained limestone			PHYLLITE: Closely spaced foliation, mica luster, but crystals not visible with handlers; SLATE: narrow spaced well developed plane of foliation, (mica is absent); HORNFELLS	RHYOLITE (3,4)	ANDESITE (3,4)	BASALT (3,4)		Fine 0.002
Amorphous	Flint, Chert		weak ROCK	strong ROCK			Mylonite	Obsidian				Amorphous
	CLASTIC				CRYSTALLINE	Organic	CRYSTALLINE					
	SILICEOUS	CALCAREOUS				Carbon -aceous	Foliated rocks may be layered or banded. This banding may be undulating or contorted, except in the case of slates where it may be exactly parallel. Metamorphic rocks often split easily along foliation planes.	Light ⇐ COLOUR ⇒ Dark; Quartz rich … Quartz poor				

GENERAL NOTES: Bedding in sedimentary rocks may not, because of its spacing, be seen in hand specimen but only in outcrop. Fossils may be found in sedimentary rocks. The mineral calcite, in calcareous rocks, may be scratched with a knife, and will react with dilute hydrochloric acid Quartz scratches steel. Broken crystals in crystalline rocks reflect light.

** siliceous and calcareous components are present (e.g. siliceous fine grained limestone)

MODE OF OCCURRENCE OF IGNEOUS ROCKS: 1. Batholiths 2. Stocks 3. Sills and dykes 4. Lava flows

* Porphyries are rocks in which some mineral grains are very much larger than the surrounding matrix. All igneous rocks can be "porphyritic".

Table 2 Identification of rock

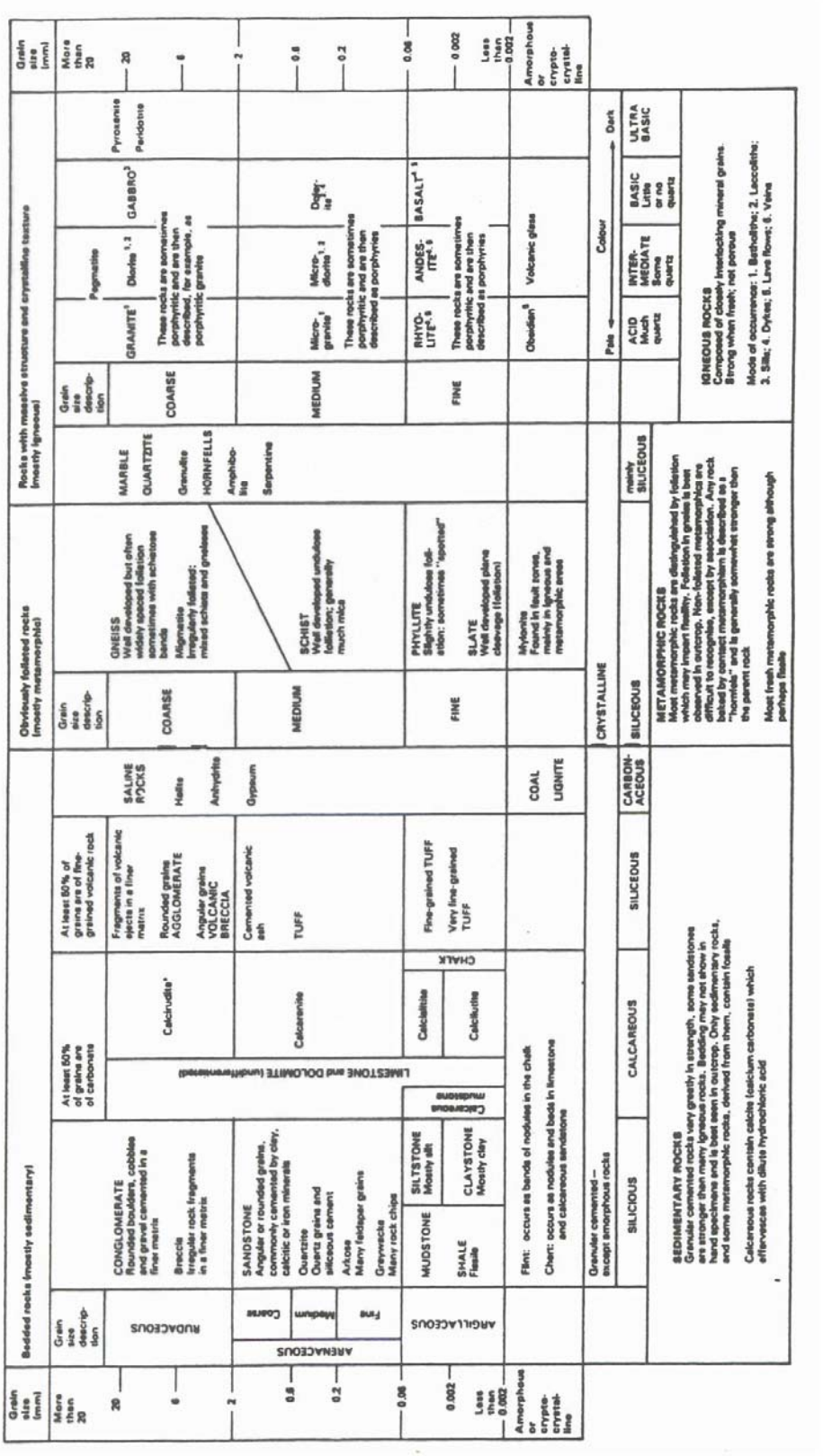

The strength of rock

When deterring the dredgebility of rock, distinction has to be made between the properties of intact rock and that of a rock mass. Depending on the fracture density of the rock the cutter will cut intact rock or break out rock blocks.
In the first case the strength (tensile- and compressive strength), deformation properties (E-value) and the petrography (mineralogical proposition) of the intact rock determines the production completely. The second case the fracture frequency and the weathering of the rock is more important than the strength of the intact rock. It is known that the absence of water in rock is important for the rock strength. When saturated with water the rock strength can be 30 to 90 % of the strength of dry rock. Therefore rock samples have to be sealed immediately after drilling in such a way that evaporation of or intake of water is avoided. It has to be mentioned that this does not mean that cutting forces in saturated rock are always lower than in dry rock.
The petrography is important for the weir of rock cutting tools

Unconfined compressive strength

The most important test for rock in the field of dredging is the unaxial unconfined compressive strength (UCS). In the test a cylindrical rock sample is axial loaded till failure. Except the force needed, the deformation is measured too. So the complete stress-strain curve is measured from which the deformation modulus and the specific work of failure can be calculated.

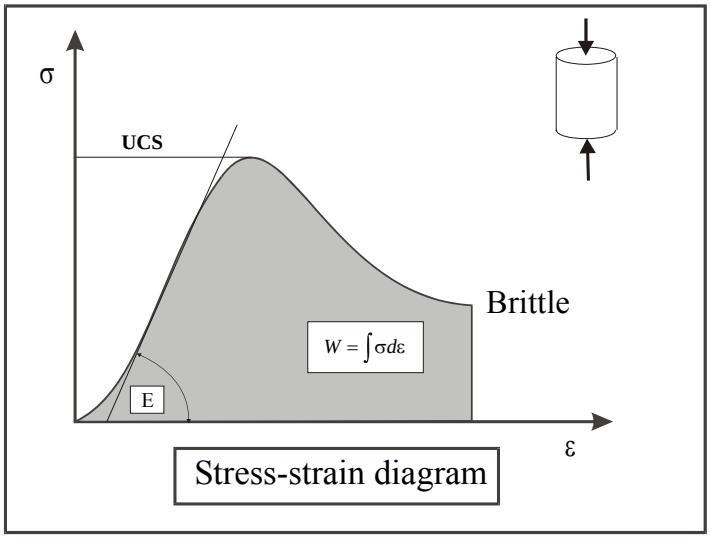

Figure 1

The compressive strength (Fig.1) is defined as: $q_u = \frac{F}{A}$ met:

q_u= the compressive strength	[N/m^2]
F = de compressive force	[N]
A = cross section of the cylinder	[m^2]
E = Deformation modulus	[N/m^2]
W = specific work of failure	[J/m^3]

Unconfined Tensile Strength

The unaxial unconfined tensile strength is defined in the same way as the compressive strength *Figure 2*a. Sample preparation and testing procedure require much effort and not commonly done Another method to determine the tensile strength , also commonly not used ,is by bending a sample *Figure 2*b

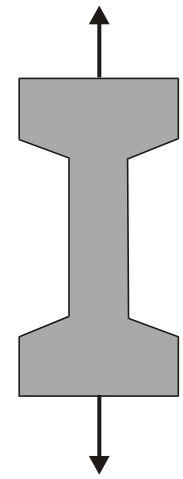

a: Unconfined

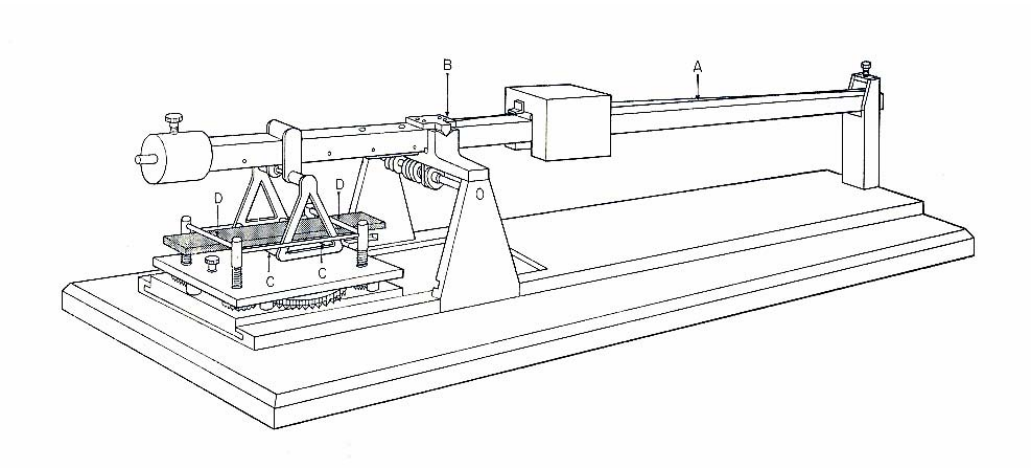

b: Bending

Figure 2

Brazilian Split Test

The most common used test to estimate, in an indirect way, the tensile strength is the Brazilian split test. Here the cylindrical sample is tested radial (Fig. 3)

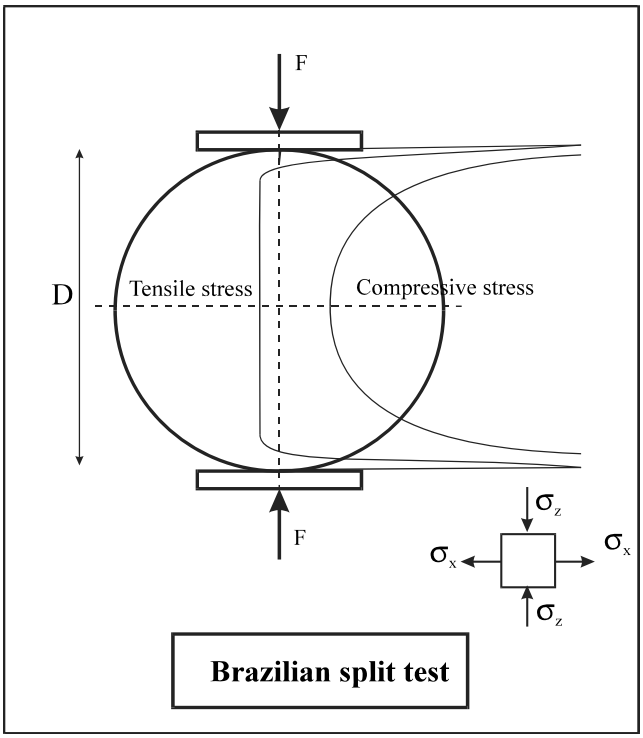

Figure 3

One can derive[Fairhurst, 1964] that the tensile stress in the centre line of the cross section is equal to: $\sigma_t = \frac{2F}{\pi Dl}$. With l the length of the sample in m., D the diameter of the sample in m. and F the compressive force in N.
The compressive force in the centre is equal to $\sigma_d = -3\sigma_t$.
The validity of BTS to determine de UTS is discussed by many researchers. In general in can be stated that the BTS over estimates the UTS. According to Pells (1993) this discussion is in most applications in practice largely academic.

Point Load test
Another test that is familiar with the Brazilian splitting test is the point load strength test (Fig. 4). This test is executed either axial, diametrical or on irregular pieces.

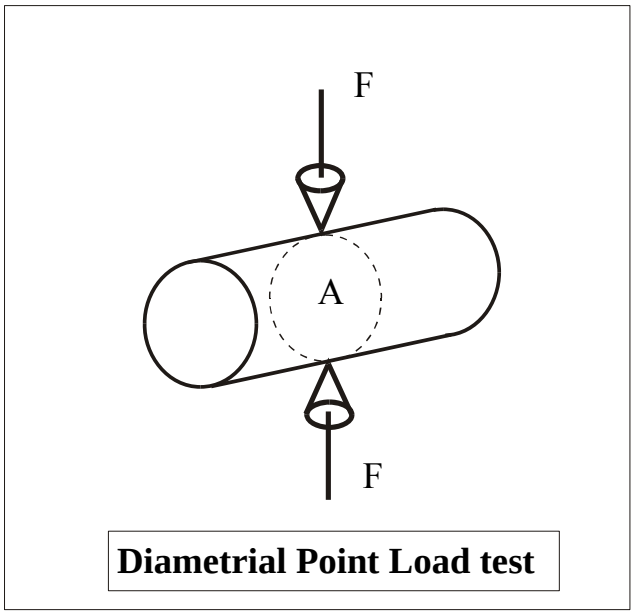

Figure 4

Point load test is frequently used to determine the strength when a large number of samples have to be tested. The tests gives for brittle rocks, when tested under diametric loading, values reasonable close to the BTS. Also it is suggested that PLS=0.8*BTS it is suggested to establish such a relation based on both tests.

Hardness

Hardness is a loosely defined term, referring the resistance to rock or minerals against an attacking tool. Hardness is determined using rebound tests (f.i. Schmidt hammer), indentation tests, (Brinell, Rockwell) or scratch tests (Mohs). The last test is based on the fact that a mineral higher in the scale can scratch a mineral lower in the scale. Although this scale was established in the early of the 19th century it appeared that the an increment of Mohs scale corresponded with a 60% increase in indentation hardness.

Table 3

Mohs Table	
No.	**Mineral**
1	Talc
2	Gypsum
3	Calcite
4	Fluorite
5	Apatite
6	Orthoglass
7	Quartz
8	Topaz
9	Corundum
10	Diamond

The failure of intact rock.

In rock failure a distinction is made between brittle, brittle ductile and ductile failure. Factors determining those types of failure are the ductility number (ratio compressive strength over tensile strength) $\frac{q_u}{\sigma_t}$, the confining pressure and the temperature. During dredging the temperature will have hardly any influence, however when drilling deep oil wells temperature will play an important role. The corresponding failure diagrams are shown in Fig. 5.
The confining pressure where the failure transit from brittle to ductile is called σ_{bp}

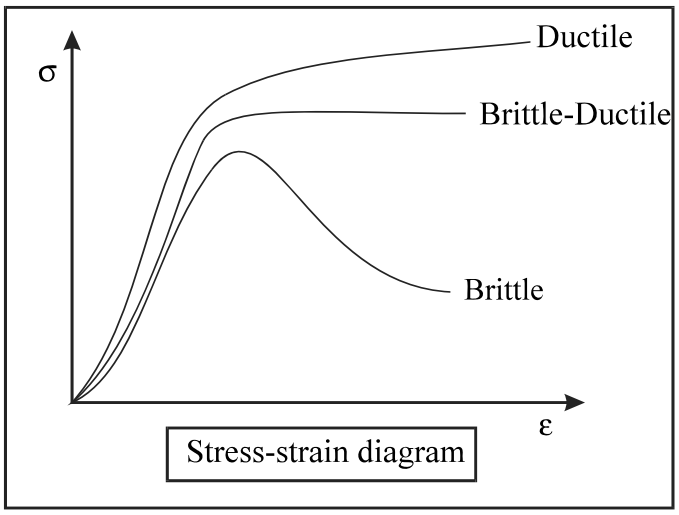

Figure 5

Brittle failure

Brittle failure occurs at relative low confining pressures $\sigma_3 < \sigma_{bp}$ en deviator stress $q=\sigma_1-\sigma_3 > \frac{1}{2}q_u$.

De strength increases with the confining pressure but decreases after the peak strength to a residual value. The presence of pore water can play an important role.

Brittle failure types are shown in Fig. 6

- Pure tensile failure with or without a small confining pressure.
- Axial tensile failure
- shear plane failure

Brittle ductile failure also called Semi brittle

In the transition area where $\sigma_3 \approx \sigma_{bp}$, the deformation are not restricted to local shear planes or fractures but are divided over the whole area. The residual- strength is more or less equal to the peak strength.

Ductile failure

A rock fails ductile when $\sigma_3 >> q_u$ en $\sigma_3 > \sigma_{bp}$ while the force stays constant or increases some what with increasing deformation

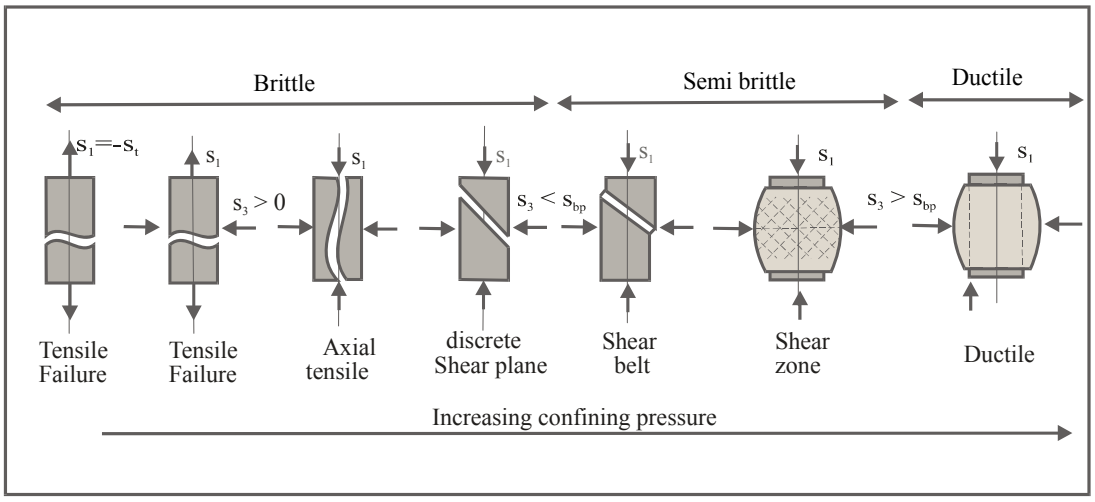

Figure 6

Failure modes in soil cutting.

In granular materials three basic failure modes can be distinguished:

- ductile (Flow Type)
- deformation in a shear plane (Shear Type)
- deformation in cracks (Tear type)

Theoretically these three failure modes can occur in all soil types.
As shown in *Figure 6* the occurrence of a particular failure mechanism is determined by external conditions as confining pressure but also from the process scale length and water depth.

In reality these basic failure modes can occur together during cutting of rock with a cutting tool as shown in *Figure 7*

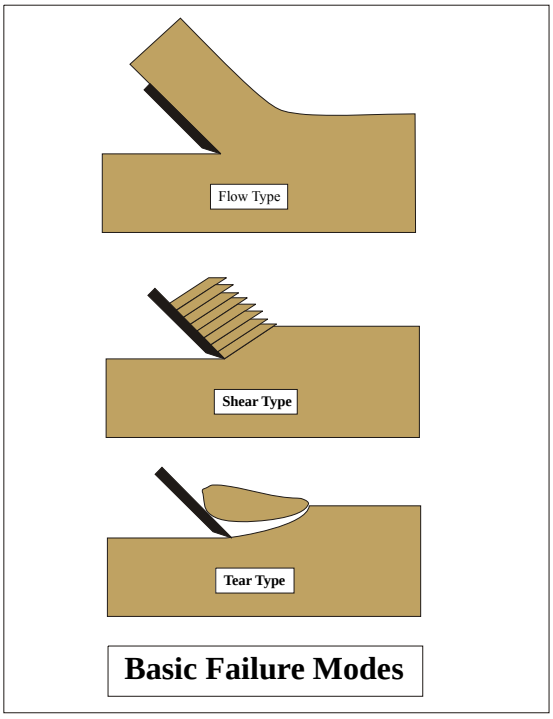

Figure 7

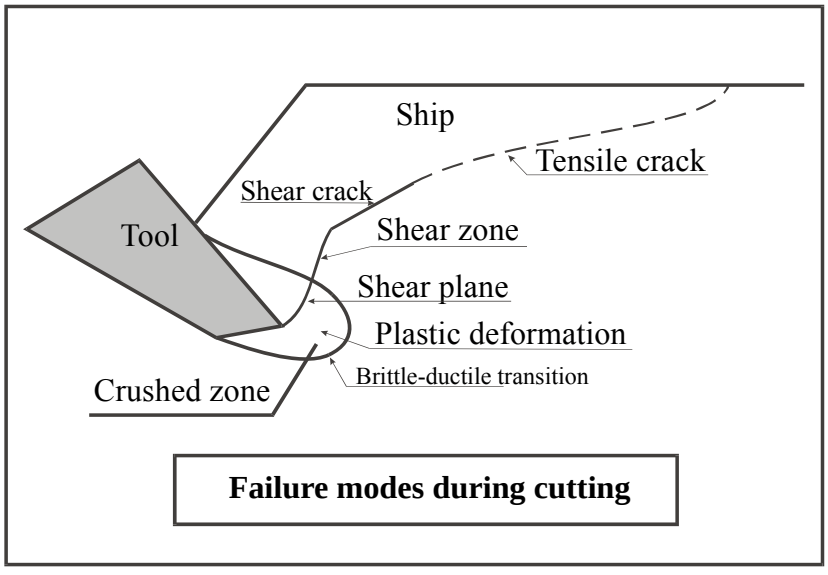

Figure 8

When cutting a crushed zone occurs under the point of the tool. At small cutting depth the crushed material will flow to the surface along the rake plane. When the depth is increased to a level that no crushed material can flow to the surface the stresses in the crushed zone will increase strongly. According to Fairhurst the cutting forces are transmitted via particle – particle

contact, forming load bearing alignments, to the environment forming. So the cutting forces transmitted to the intact rock as discrete point loads, causing micro cracks and finally in a tensile crack.

In this cutting process the following failure types occurs according Fig. 8.
Traject I: a tensile failure
Traject II: a shear failure
Traject III a shear bend or area
Traject IV plastic deformation

The transition of brittle to ductile is still a point of investigation. For the time being it is assumed that the confined pressure at the transition is a function of the ratio unconfined compressive strength (UCS) over the unconfined tensile strength (UTS); $m = \frac{q_u}{\sigma_t}$. See chapter envelope for ductile failure.

The influence of the failure mechanism is shown well in the cutting force registration for brittle and ductile rock as function of time as shown in figure below.

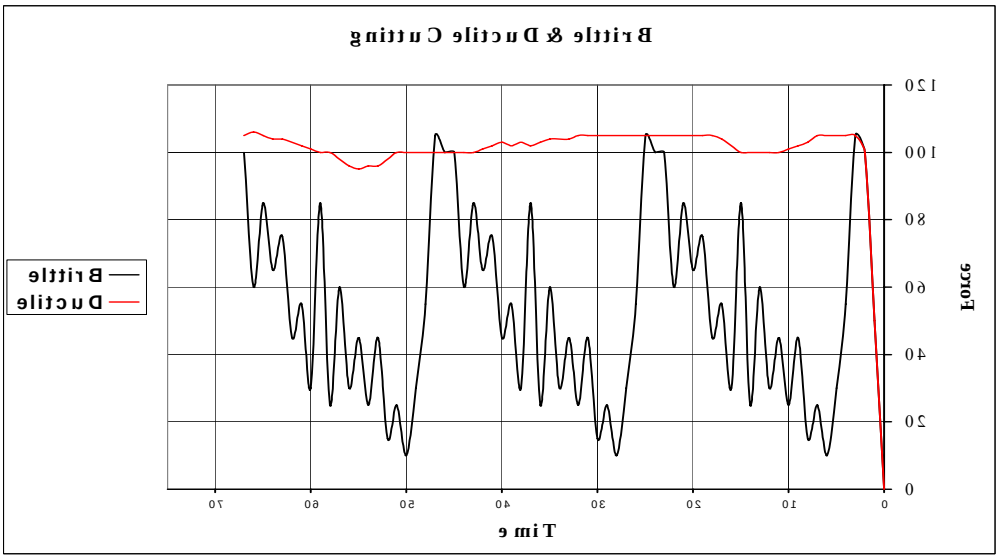

Figure 9

Cutting rock in a brittle or in a ductile mode can have influence on the type of pick to be used. Under brittle failure chips are formed with breaking out angles wider than the cross section of the tooth, β_2 positive.

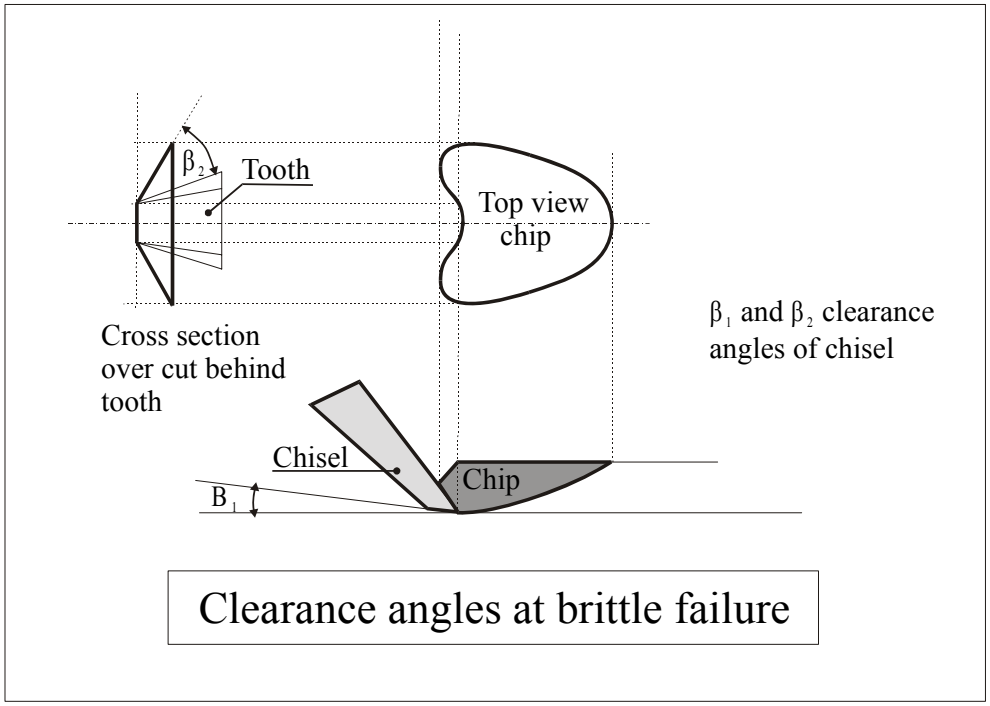

Figure 10

On the other hand when cutting in ductile mode β_2 will be negative. In that case trapezoidal pick points will be preferable.

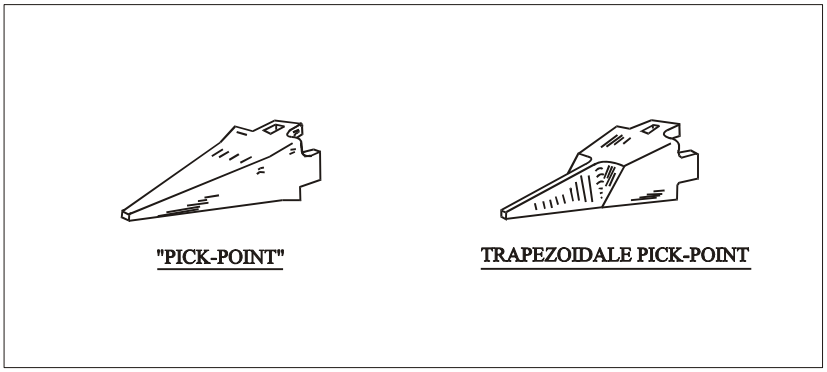

Figure 11

Failure of rock

In engineering practice a number failure criteria are known. The most important are:

- The maximum stress theory
- The maximum strain theory
- The maximum shear stress theory
- The theory of Mohr
- The theory of maximum distortion energy

Combinations of these theories are developed too.

For rock it is common to use the theory of Mohr.

Failure theory of Mohr

The failure of rock is mostly discussed with the failure model of Mohr

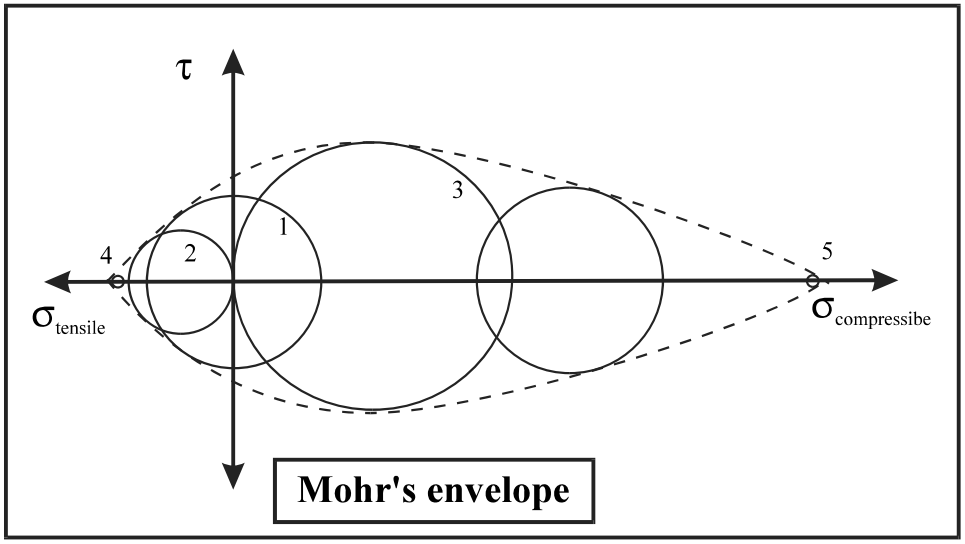

Figure 12

The difference with all other failure theories is that having executed a number of experiments it is decided where the material fails or where not.
In *Figure 12* a pure shear test (circle 1), pure tensile test (circle 2), pure compression test (3), a hydrostatic tension test (4), a hydrostatic compression tests (5) and if required a number of additional tests. Plotting the circles, which the stresses when failure occurs and enveloping those circles by curves, it is stated that for the region inside the envelope no failure will occur and on or outside the envelope, the rock start to fail or is completely failed.

In figure 13 the rock starts to fail in point A at a shear stress τ_A and a normal stress σ_A. The main stresses at this point are σ_1 and σ_3
The relation between τ and σ_1-σ_3 and σ and σ_1+σ_3 can easily derived.

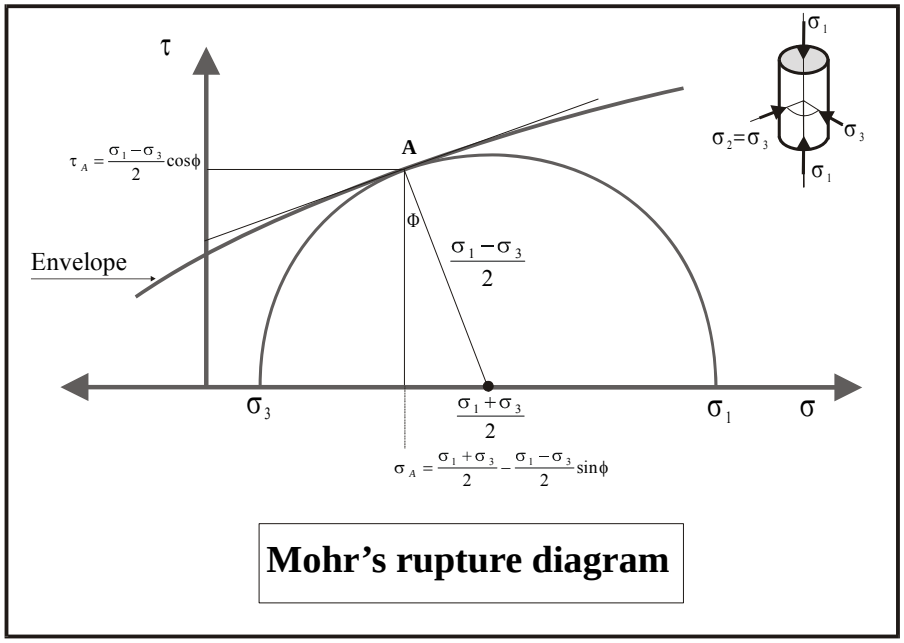

Figure 13

The envelope in this τ-σ diagram can be transformed to the σ_1-σ_3 diagram, giving the relation between σ_1 and σ_3 when failure starts. Such a diagram shows for the required minimum main stress as function of the confining pressure to get failure.

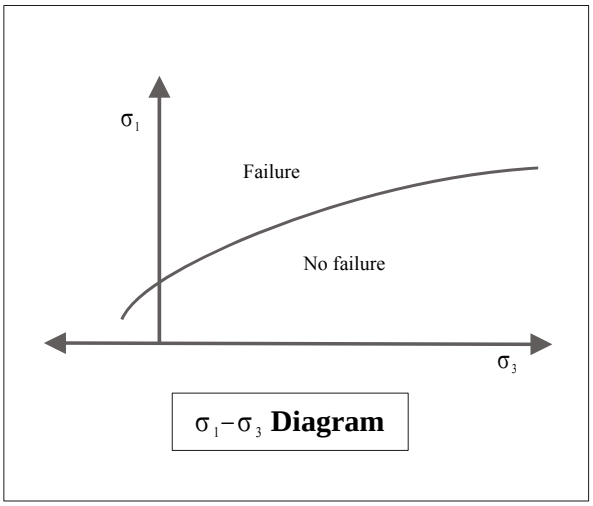

Figure 14

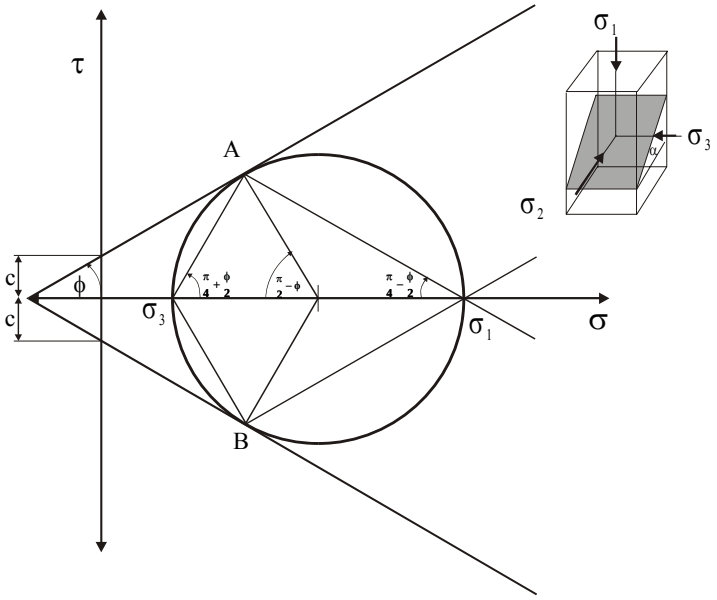

Figure 15

Dependant on the main stress the failure makes an angle $\frac{\pi}{4}+\frac{\phi}{2}$ or $\frac{\pi}{4}-\frac{\phi}{2}$ with the horizontal axes. In principal the failure makes an angle $\frac{\pi}{4}-\frac{\phi}{2}$ with the direction of the main stress.

Besides the σ_1-σ_3 diagram, use is also made from the p-q diagram, in which $p=(\sigma_1+\sigma_2+\sigma_3)/3$ is called the hydrostatic stress and $q=\sigma_1-\sigma_3$ the deviator stress. σ_1-σ_3 equals 2 times the radius of Mohr's circle, while mostly during test $\sigma_2=\sigma_3$, so $_p=(\sigma_1+2\sigma_3)/3$.

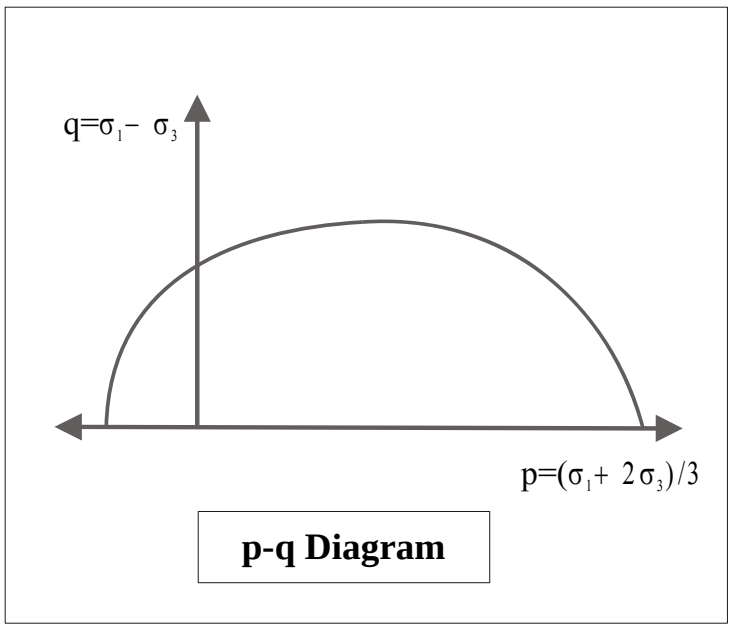

Figure 16

Remark.
The crossing of the envelope with the x-axes gives on the right side hydrostatic pressure and on the left side hydrostatic tension.

For rock a distinction is made for different type of failures, brittle, ductile or brittle-ductile or semi brittle. So use is made of different parts of the envelope of Mohr.
The envelope for brittle failure is mainly determined by the peak stresses of the rock and can be determined by the Brazilian split test and a number of compression tests in a triaxial apparatus with different confining pressures.
Depending on what kind of tests are done the literature make use of different Mohr's envelopes for brittle failure.

Envelopes for brittle failure

1. Linear envelope tangent to the axial tension circle en uniaxial compression circle.

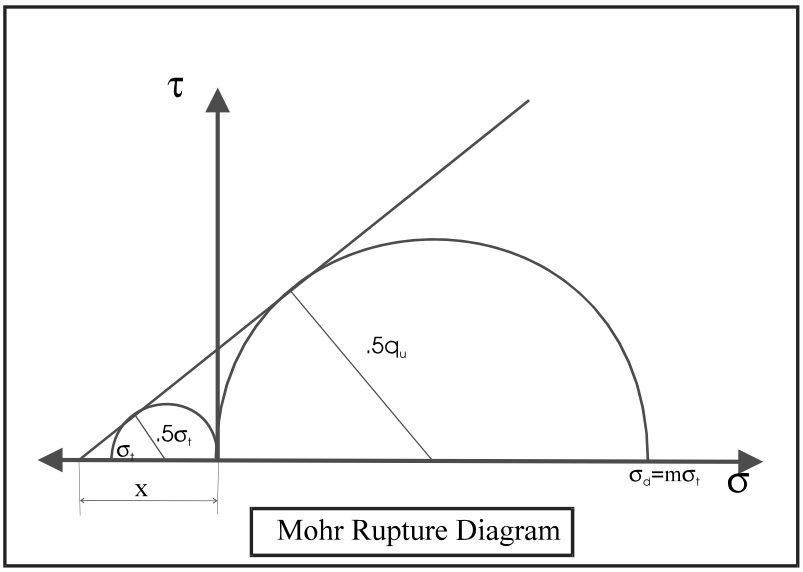

Figure 17

The general equation is $\tau = c + \sigma \tan\phi$
From Figure 17 follows that

$$\tau = \frac{\sigma_1 - \sigma_3}{2}\cos\phi$$

$$\sigma = \frac{\sigma_1 + \sigma_3}{2} - \frac{\sigma_1 - \sigma_3}{2}\sin\phi$$

Substituted in the general equation gives:

$$\frac{\sigma_1-\sigma_3}{2}\cos\phi = c + \left[\frac{\sigma_1+\sigma_3}{2} - \frac{\sigma_1-\sigma_3}{2}\sin\phi\right]\tan\phi$$

or $$\frac{\sigma_1-\sigma_3}{2}\cos^2\phi = c\cos\phi + \frac{\sigma_1+\sigma_3}{2}\sin\phi - \frac{\sigma_1-\sigma_3}{2}\sin^2\phi$$

$$\frac{\sigma_1-\sigma_3}{2} = c\cos\phi + \frac{\sigma_1+\sigma_3}{2}\sin\phi$$
$$\sigma_1-\sigma_3 = 2c\cos\phi + \sigma_1\sin\phi + \sigma_3\sin\phi$$

resulting in

$$\sigma_1 = \sigma_3\frac{(1+\sin\phi)}{(1-\sin\phi)} + 2c\frac{\cos\phi}{(1-\sin\phi)} = \sigma_3\frac{(1+\sin\phi)}{(1-\sin\phi)} + 2c\sqrt{\frac{(1+\sin\phi)}{(1-\sin\phi)}}$$

This equation can be written as:

$$\sigma_1 = \sigma_3\tan^2\left(\frac{\pi}{4}+\frac{\phi}{2}\right) + 2c\tan\left(\frac{\pi}{4}+\frac{\phi}{2}\right)$$

The general equation $\tau = c + \sigma\tan\varphi$ can be expressed in the compressive strength q_u and the ratio between the compressive strength and the tensile strength m

From Figure 17 follows that $\sin\phi = \frac{q_u-\sigma_t}{q_u+\sigma_t}$

And according Figure 18 : $\cos\phi = \frac{\sqrt{q_u\sigma_t}}{q_u+\sigma_t}$ en $\tan\phi = \frac{q_u-\sigma_t}{2\sqrt{q_u\sigma_t}}$

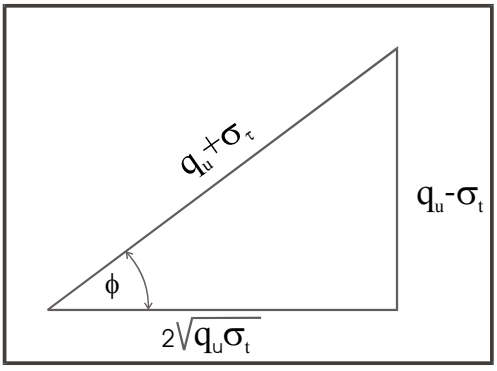

Figure 18

Further more follows from Figure 17 :

$$\frac{x-\frac{\sigma_t}{2}}{x+\frac{q_u}{2}}=\frac{\frac{\sigma_t}{2}}{\frac{q_u}{2}} \Rightarrow \frac{q_u}{2}\cdot\left(x-\frac{\sigma_t}{2}\right)=\frac{\sigma_t}{2}\left(x+\frac{q_u}{2}\right) \Rightarrow \; x=\frac{\sigma_t q_u}{q_u-\sigma_t}$$

and $c=\dfrac{x}{\tan\phi}$ or $c=\dfrac{x}{\tan\phi}=\dfrac{\sigma_t q_u}{\frac{q_u-\sigma_t}{\tan\phi}}=\dfrac{\sigma_t q_u}{q_u-\sigma_t}\dfrac{q_u-\sigma_t}{2\sqrt{\sigma_t q_u}}=\dfrac{1}{2}\sqrt{\sigma_t q_u}$

This results with $m=\dfrac{q_u}{\sigma_t}$ in $\tau=c+\sigma\tan\phi$:

$$\frac{\tau}{q_u}=\frac{1}{2\sqrt{m}}+\frac{\sigma}{q_u}\cdot\frac{m-1}{2\sqrt{m}} \qquad \text{met } m=\frac{q_u}{\sigma_t}$$

and in the σ_1 - σ_3 diagram

$$\frac{\sigma_1}{q_u}=\frac{1}{m}+m\frac{\sigma_3}{q_u}$$

Giving a linear relation between $\dfrac{\sigma_1}{q_u}$ and $\dfrac{\sigma_3}{q_u}$

2. Linear envelope tangent to the Brazilian tension circle en unaxial compression circle.

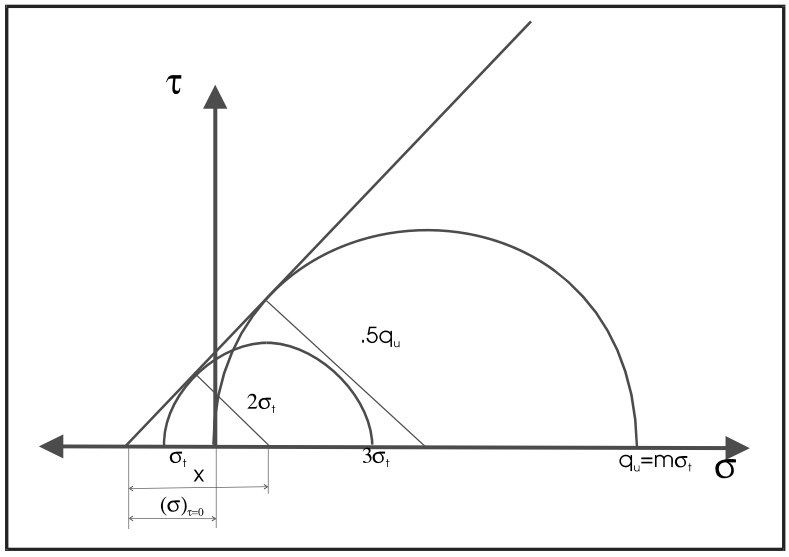

Figure 19

In the same way one can derive:

$$\frac{\tau}{q_u}=\frac{1}{2\sqrt{m-3}}+\frac{m-4}{2\sqrt{m-3}}\frac{\sigma}{q_u}$$

$$\frac{\sigma_1}{q_u} = \frac{4-m}{2-m} + (3-m)\frac{\sigma_3}{q_u}$$

3. Parabolic envelope tangent to the unaxial tension circle en unaxial compression circle.

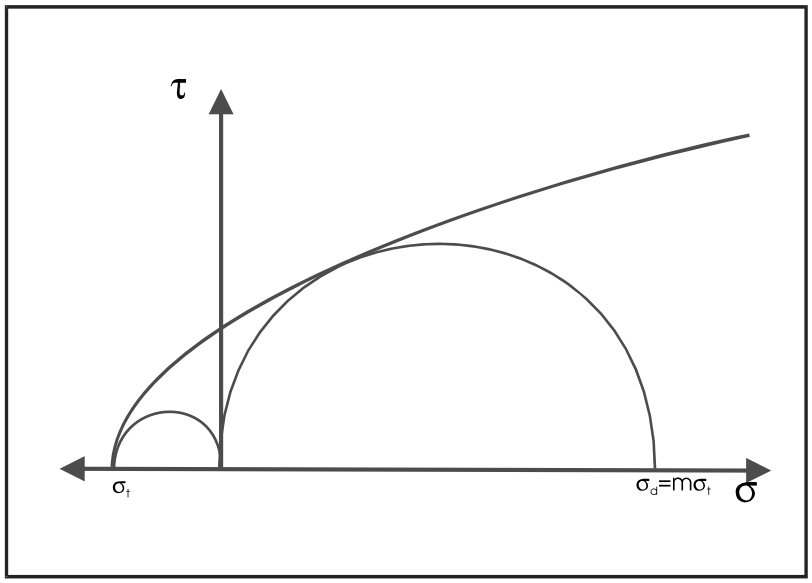

Figure 20

The equation of the envelope is: $\tau^2 = \sigma_t\left(\sqrt{m+1}-1\right)^2(\sigma+\sigma_t)$

and

$$\frac{\sigma_1-\sigma_3}{q_u} = \frac{\sqrt{m+1}-1}{m}\left\{\sqrt{m+1}-1+2\sqrt{m\frac{\sigma_3}{q_u}+1}\right\}$$

This type of envelope is used by Griffith.
Griffith (Fairhurst, 1964) has derived a criterion for **brittle failure**. His hypothesis assumes that fracture occurs by rapid extension of sub-microscopic, pre-existing flaws, randomly distributed throughout the material.
He defined the following criteria:

- If $3\sigma_1 + \sigma_3 \geq 0$, failure will occur when $\sigma_1=\sigma_t$; the unaxial tensile strength. (Remember; The condition $3\sigma_1+\sigma_3=0$ is fulfilled in the Brazilian split test)

- And when $3\sigma_1 + \sigma_3 \leq 0$, failure will occur when $(\sigma_1-\sigma_3)^2 + 8\sigma_t(\sigma_1+\sigma_3) = 0$
  In the τ-σ diagram the Mohr envelope for this criteria is the parabola: $\tau^2 = 4\sigma_t(\sigma_t-\sigma)$

From the second criteria one can derive that brittle failure will occurs when the ratio of uniaxial compressive strength over uniaxial tensile strength is 8 or higher. (put $\sigma_3=0$, this gives $\sigma_1=-8\ \sigma t$. So for the unconfined compressive strength test $\sigma_3=0$ and $\sigma_1=qu=-8\ \sigma_t$)

Fairhurst gives in his article a empirical generalisation of Griffith criterion to overcome the critic of the constant ratio $\frac{q_u}{\sigma_t}$=8. He stated :

- If $n(2n-1)\sigma_1 + \sigma_3 \geq 0$, failure will occur when $\sigma_1=\sigma_t$; the unaxial tensile strength
- If $n(2n-1)\sigma_1 + \sigma_3 \leq 0$, failure will occur when:

$$\frac{(\sigma_1 - \sigma_3)^2}{\sigma_1 + \sigma_3} = -2n(n-1)^2 \sigma_t \left[1 + \frac{2\sigma_t}{\sigma_1 + \sigma_3} \left\{ \left(\frac{n-1}{2} \right)^2 - 1 \right\} \right]$$

With $n = \sqrt{(m+1)}$ and m=$\frac{q_u}{\sigma_t}$, the absolute value of the unaxial compressive strength over the unaxial tensile strength.

In the dredging technology the specific energy formulas are mostly based on the compressive strength of rock and are of the condition $SPE=A \cdot g(f_i) \cdot q_u$.
In which A is a constant $g(f_i)$ a value depending on the fracture spacing index and q_u the unconfined compressive strength.
When this value is based on rocks with small m-values it will over estimate the SPE for rocks with large m-values. Of coarse if the SPE is based on high m-values it will under estimate the SPE for small m-values.

4. The brittle failure envelope according Hoek & Brown
Hoek & Brown have developed from experiments on rocks with different tension-compression ratio's a relation between the main stresses for brittle failure.

$$\frac{\sigma_1 - \sigma_3}{q_u} = \sqrt{m\frac{\sigma_3}{q_u} + 1}$$

This equations gives parabola in the σ_1-σ_3 diagram.

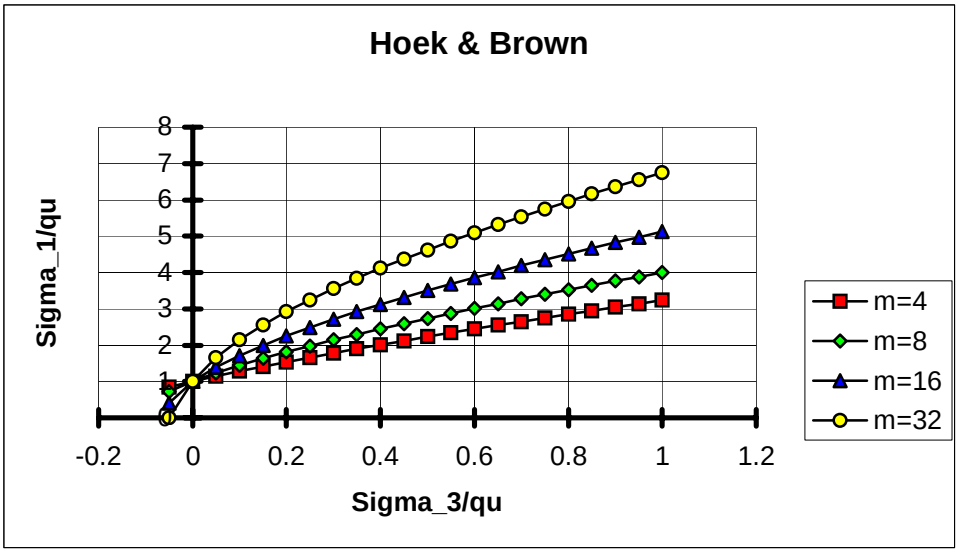

Figure 21

In the τ–σ diagram the equation is given in parameter form:

$$\frac{\tau}{q_u} = \frac{1}{2}\sqrt{m\frac{\sigma_3}{q_u}+1}\cdot\sqrt{1-\left(\frac{m}{m+4\sqrt{m\frac{\sigma_3}{q_u}+1}}\right)^2}$$

$$\frac{\sigma}{q_u} = \frac{\sigma_3}{q_u}+\frac{1}{2}\sqrt{m\frac{\sigma_3}{q_u}+1}\left[1-\frac{m}{m+4\sqrt{m\frac{\sigma_3}{q_u}+1}}\right]$$

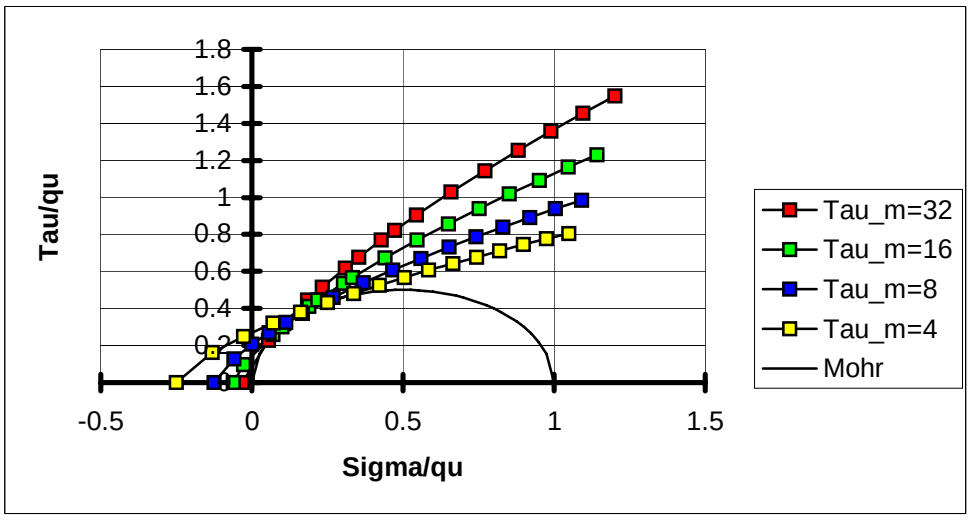

Figure 22

Because this envelope is based on a large number of tests, it is preferable above the other equations.
An estimation about the m-value for common rocks can be found in the table below. (Hoek et al. 1995)

Table 4

Rock type	Class	Group	Texture			
			Coarse	Medium	Fine	Very fine
Sedimentary	Clastic		Conglomerate (22)	Sandstone 19	Siltstone 9	Claystone 4
			<----Greywacke----> (18)			
	Non-clastic	Organic	<------Chalk------> 7 <------Coal-------> (8-21)			
		Carbonate	Breccia (20)	Sparitic Limestone[1] 10	Micritic Limestone[2] 8	
		Chemical		Gypsum 16	Anhydrite 13	
Metamorphic	Non foliated		Marble 9	Hornfels (19)	Quartzite 24	
	Slightly foliated		Migmatite (30)	Amphibolite 31	Mylonite (6)	
	Foliated[3]		Gneiss 33	Schist (10)	Phyllites (10)	Slate 9
Igneous	Light		Granite 33 Granodiorite (30) Diorite 28 Gabbro 27 Norite 22	Dolerite (19)	Rhyolite (16) Dacite (17) Andesite 19 Basalt (17)	Obsidian (19)
	Extrusive pyroclastic type		Aggomerate (20)	Breccia (18)	Tuff (15)	

The envelope for ductile failure.
Mogi (1966) found in his research on certain types of rock a linear relation between the main stresses for transition between brittle and ductile. For sandstone $\sigma_1 = 3.4\sigma_3$ and for limestone $\sigma_1 = 4.2\sigma_3$ Those values can only be an indication, because other researches found, especially, for limestone higher values for the transition between brittle and ductile (Verhoef $\frac{\sigma_1}{\sigma_3} \geq 6$

As stated earlier the transition between brittle and ductile is assumed to be a function of the ratio UCS over UTS.

If it is assumed that for brittle failure the theory of Hoek & Brown is valid $\frac{\sigma_1 - \sigma_3}{q_u} = \sqrt{m\frac{\sigma_3}{q_u} + 1}$ together with Mogi's theory $\sigma_1 = \alpha\sigma_3$, then the confined strength can be calculated for the intersection of the lines.

Indeed the confined pressure at the transition between brittle and ductile is only depended on the ratio UCS over UTS when the theory of Mogi is valid. The results are presented in the graph below for different values of α

$$\frac{(\alpha-1)\sigma_3}{q_u}=\sqrt{m\frac{\sigma_3}{q_u}+1}\ \Rightarrow\ (\alpha-1)^2\left(\frac{\sigma_3}{q_u}\right)^2=m\frac{\sigma_3}{q_u}+1$$

$$\frac{\sigma_3}{q_u}=\frac{m\pm\sqrt{m^2+4(\alpha-1)^2}}{2(\alpha-1)^2}$$

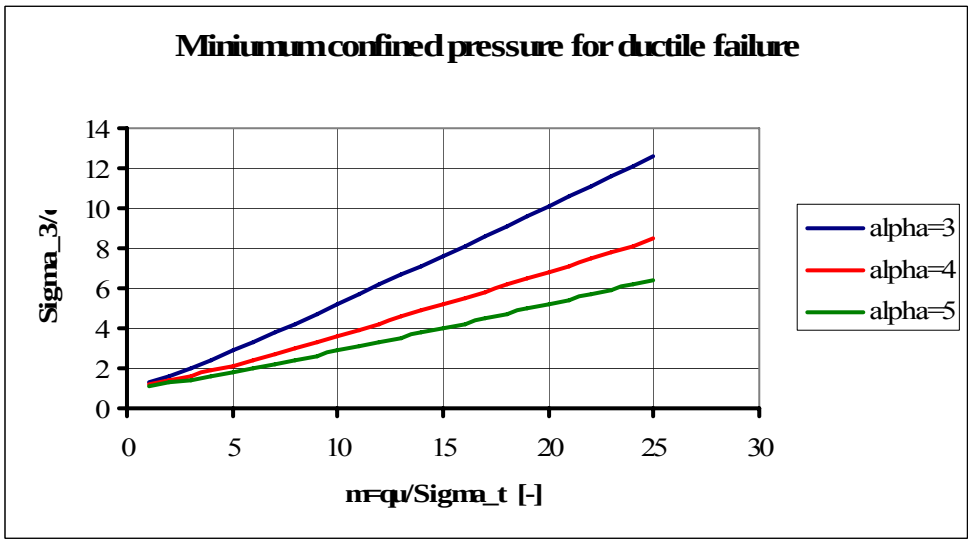

Figure 23

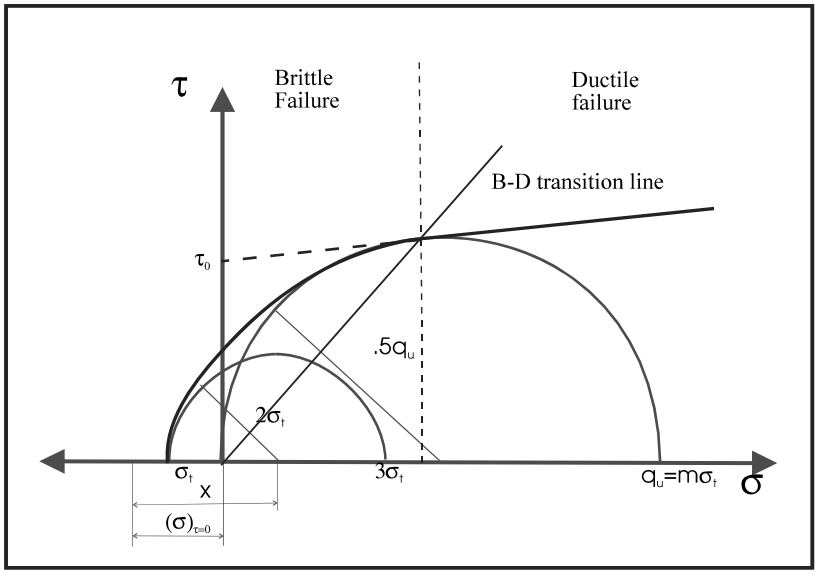

Figure 24

The slope of the envelope in the ductile area is determined either the cutting process is drained or undrained. In drained conditions pore water flow is possible due to pressure gradients. In undrained conditions pore water flow is not possible and the pore water pressure will affect the

stress state in the pores. Which condition occurs depends on the speed of failure and the permeability.
Under drained conditions the slope of the envelope can be estimated from the slope from the brittle envelope at the transition point of brittle – ductile. Undrained cutting of rock can be compared with cutting of clay and metal. In this case the slope of the envelope $\phi=0$.
Van Kesteren (1995) stated that pore water pressures must play a role in the formation of the crushed zone. He distinguished to limiting conditions; drained and undrained. In the drained situation a pore water flow is possible due to the pressure gradient in the pores without hindering the volume change behaviour due to the change in the stress state. In the undrained state migration of pore water is virtually impossible. No volume change will occur in the material of the intact rock that becomes a part of the crushed zone. In the crushed zone the total isotropic total stress is very high with the result that the pore pressure is very high too

As showed above the transition between brittle and ductile failure is mainly determined by the ratio $\frac{q_u}{\sigma_t}$. So stated Gehring (1987) that ductile failure will occur when the ratio $\frac{q_u}{\sigma_t} < 9$ and brittle failure when $\frac{q_u}{\sigma_t} > 15$, while $9<\frac{q_u}{\sigma_t}<15$ the rock fails in the transition between brittle and ductile. These values are in agreement with the theory of Fairhurst (Fairhurst, 1964)

Influence of water depth

Weak brittle rocks have tensile strength of 0.2 to 5 Mpa. The maximum pressure differences that can occur in the cracks when cavitation occurs depends on the water depth and is in the order of 0.2 to 0.4 Mpa for 10 to 30 m water depth.
Therefore the influence of the water depth on the crack propagation is limited.
In the case of very thin fracture it might be possible that due to the capillary action of the pore water cavitation does not occur, which will increase the cutting forces.

The influence of discontinuities

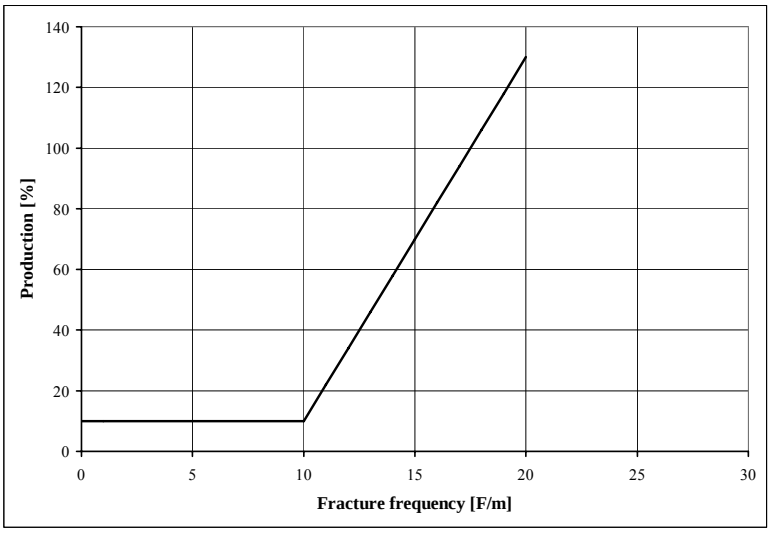

Figure 25

The presents of fracture influence the dredgebility of rock strongly. If the fracture frequency is that high that the block size is in the order of the maximum cutting depth of the cutting tools, the rock strength plays a less important role for the production than when the fracture frequency results in block sizes in the size of the cutting tool.
When drilling ores in rock the driller determines the RQD-value of the rock. This is the percentage of drill samples with a length of 10 cm or more per meter core length. The RQD value is only a rough estimate of the fracture frequency.

Besides the fracture frequency the decomposition or weathering of the rock is a important parameter for the dredgebility.
The decomposition is expressed in grades.

Table 5

Grade I	fresh or intact rock	(Intact gesteente)
Grade II	slightly decomposed	(Licht verweerd)
Grade III	Moderately decomposed	(Matig verweerd)
Grade IV	Highly decomposed	(Sterk verweerd)
Grade V	Completely decomposed	(Volledig verweerd)
Grade VI	Residual soil	Residue (gesteente)

The difference between completely decomposed and residual soil is the original rock structure is present in the first and not in the last.
Except the production the cutting tool consumption per m^3 dredged soils depends on these factures too.

Simple cutting models

For the cutting models discussed in this chapter, the following assumptions are made:

- The width of the cutting tools is much larger than the depth of the (B>>d), so 2D cutting theories.
- The state of the plane stress is valid

I. Model of Evans

Evans suggested a model on basis of observations on coal breakage by wedges.
In this theory it is assumed that:

- a force R is acting under an angle φ with the normal to the surface ac of the wedge.
- A Resultant force T of the tensile forces acting at right angles on the arc cd
- A third force S is required to maintain equilibrium in the buttock.
- The penetration of the wedge is small compared to the thickness d

The action of the wedge tends to split the rock and does rotate it about point D. It is therefore assumed that the force S acts through D.
Along the fracture it is assumed that a state of plain strain is working and the equilibrium is considered per unit of width of the rock .

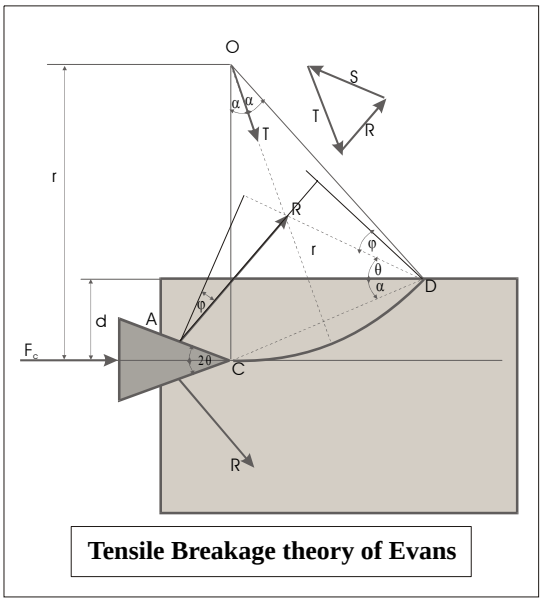

Figure 26

The force due to the tensile strength of the rock is: $T = \sigma_t r \int_{-\alpha}^{\alpha} \cos\omega d\omega = 2\sigma_t r \sin\alpha$

where rdω is an element of the arc CD making an angle ω with the symmetry - axe of the arc.
Let d be the depth of the cut and assume that the penetration of the edge may be neglected in comparison with d. This means that the force R is acting near point C.
Taking moments about D gives

$$R\frac{d}{\sin\alpha}\cos(\alpha+\theta+\varphi) = Tr\sin\alpha$$

From the geometric relation follows: $r\sin\alpha = \frac{d}{2\sin\alpha}$ hence $R = \frac{\sigma_t d}{2\sin\alpha\cos(\alpha+\theta+\varphi)}$.

The horizontal component of R is Rsin(θ+φ) en due to the symmetry of the forces acting on the wedge the total cutting force is:

$$F_c = 2R\sin(\theta+\varphi) = \frac{d\sigma_t \sin(\theta+\varphi)}{\sin\alpha\cos(\alpha+\theta+\varphi)}$$

The normal force (⊥ on cutting force) is per side:

$$F_n = R\cos(\theta+\varphi) = \frac{d\sigma_t \cos(\varphi+\varphi)}{\sin\alpha\cos(\alpha+\theta+\varphi)}$$

The assumption is made that α is determined in such that F_c is minimal, i.e. that $\frac{dF_c}{d\alpha} = 0$ giving:

$$\cos\alpha\cos(\alpha+\theta+\varphi)-\sin\alpha\sin(\alpha+\theta+\varphi)=0\Rightarrow\cos(2\alpha+\theta+\varphi)=0$$

Resulting in $\alpha=\frac{1}{2}\left(\frac{\pi}{2}-\theta-\varphi\right)$ or

$$\sin\alpha\cos(\alpha+\theta+\varphi)=\sin\left(\frac{1}{2}\left[\frac{\pi}{2}-\theta-\varphi\right]\right)\cos\left(\frac{1}{2}\left[\frac{\pi}{2}+\theta+\varphi\right]\right)=\frac{1}{2}\left[\sin\left(\frac{\pi}{2}\right)-\sin(\theta+\varphi)\right]$$

hense:

The total cutting $F_c=\frac{2d\sigma_t\sin(\theta+\varphi)}{1-\sin(\theta+\varphi)}$

and

The normal force ⊥ F_c for one side $F_n=R\cos(\theta+\varphi)=\frac{d\sigma_t\cos(\theta+\varphi)}{1-\sin(\theta+\varphi)}$ but the total normal force is zero due to the symmetry

If the friction between the rock an d R is zero φ=0 and the cutting force reduces to:

$$F_c=\frac{2d\sigma_t\sin(\theta)}{1-\sin(\theta)} \text{ and } F_n=0$$

N.B.

All forces are per unit of width!

The standard tooth

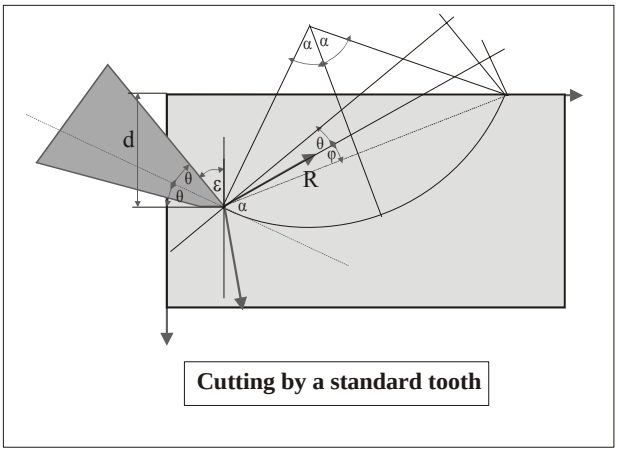

Figure 27

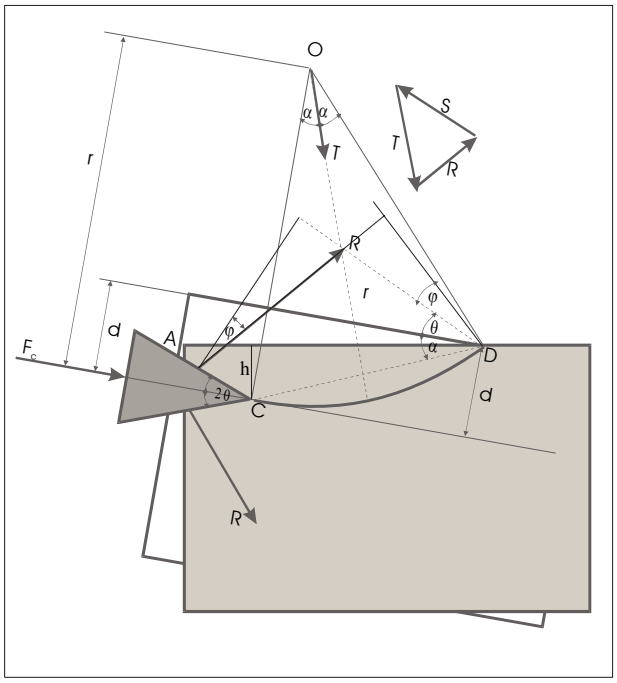

Figure 28

For a standard tooth one can derive with the aid of: Figure 28.

$h = 2r\sin\alpha \cdot \sin(\alpha - \varepsilon)$ *and* $d = 2r\sin^2\alpha$

or

$$d = h\frac{\sin\alpha}{\sin(\alpha - \varepsilon)}$$

$$F_c = \frac{2d\sigma_t \sin(\theta+\varphi)}{1-\sin(\theta+\varphi)} = \frac{2h\sigma_t \sin\alpha}{\sin(\alpha-\varepsilon)} \cdot \frac{\sin(\theta+\varphi)}{1-\sin(\theta+\varphi)}$$

The horizontal component will be:

$$[F_c]_h = \frac{2h\sigma_t \sin\alpha}{\sin(\alpha-\varepsilon)} \cdot \frac{\sin(\theta+\varphi)}{1-\sin(\theta+\varphi)} \cos\varepsilon$$

and the vertical component:

$$[F_c]_v = \frac{2h\sigma_t \sin\alpha}{\sin(\alpha-\varepsilon)} \cdot \frac{\sin(\theta+\varphi)}{1-\sin(\theta+\varphi)} \sin\varepsilon$$

The above equation is only valid when the path of the cutting tool has the same direction as the fracture. This means that if the maximum thickness of the chip is almost the cutting depth that this expression can be used.

For a horizontal moving cutting tool the same equation can be used under the condition that $\theta = \frac{1}{2}[\pi/2 - \varepsilon]$. Physical this means that the cutting tools has a horizontal wear flat and the therefore a wedge angle of $\pi/2-\varepsilon$. Note that $F_n = [F_c]_v$ is not zero anymore**.**

Figure 29

In practice teeth will have always a wear flat. Assuming that wear flat is parallel with the transverse direction, the total force on the wear flat equals $R_w=R_t$ and the bisector of the wedge makes angles θ with the wedge sides according to Figure 30

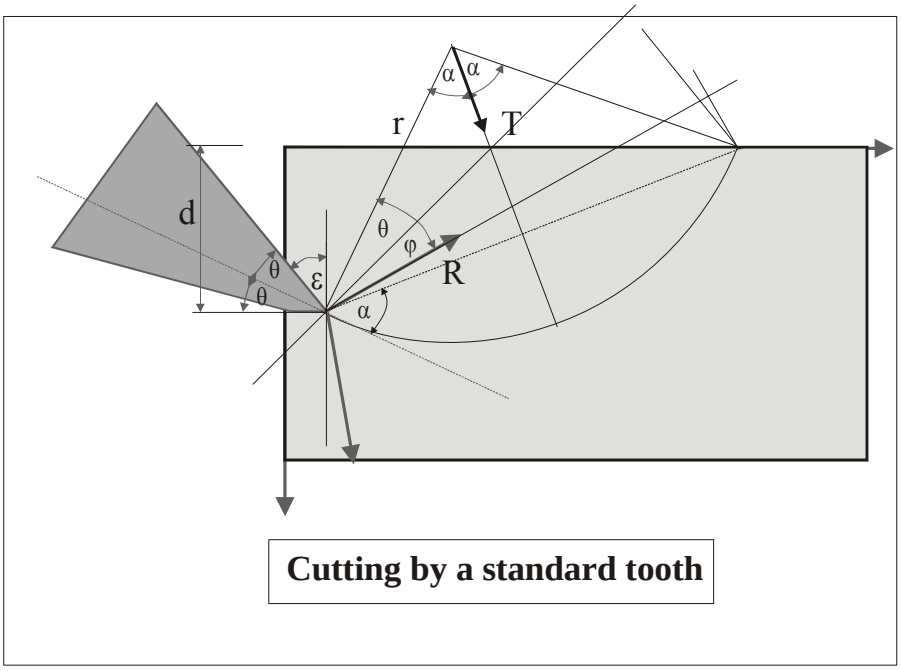

Figure 30

Taking again the moments about D

$$R_t \frac{d}{\sin(\alpha-\theta)}\cos(\alpha+\theta+\varphi) = Tr\sin\alpha$$

From the geometric relation follows: $r\sin\alpha = \dfrac{d}{2\sin(\alpha-\theta)}$ hence:

$$R_t = \frac{\sigma_t d}{2\sin(\alpha-\theta)\cos(\alpha+\theta+\varphi)} = R_w .$$

The total force F is:

$$F = 2R\cos\left[\alpha+\left(\frac{\pi}{2}-\alpha-\theta-\varphi\right)\right] = 2R\sin(\theta+\varphi)$$

$$F = \frac{\sigma_t d\sin(\theta+\varphi)}{\sin(\alpha-\theta)\cos(\alpha+\theta+\varphi)}$$

The assumption is made that α is determined in such that F_c is minimal, i.e. that $\frac{dF}{d\alpha}=0$ changes to: $\cos(\alpha-\theta)\cos(\alpha+\theta+\varphi)-\sin(\alpha-\theta)\sin(\alpha+\theta+\varphi)=0 \Rightarrow \cos(2\alpha+\varphi)=0$

Resulting in $2\alpha+\varphi=\frac{\pi}{2}$ or $\alpha=\frac{\pi}{4}-\frac{\varphi}{2}$

And hence

$$F=\frac{\sigma_t d\sin(\theta+\varphi)}{\sin\left(\frac{\pi}{4}-\theta-\frac{\varphi}{2}\right)\cos\left(\frac{\pi}{4}+\theta+\frac{\varphi}{2}\right)}=\frac{\sigma_t d\sin(\theta+\varphi)}{\frac{1}{2}\left[\sin\left(\frac{\pi}{2}\right)-\sin(2\theta+\varphi)\right]}$$

$$F=\frac{2\sigma_t d\sin(\theta+\varphi)}{1-\sin(2\theta+\varphi)}$$

The cutting force F_c becomes:

$$F_c=\frac{2\sigma_t d\sin(\theta+\varphi)\cos\theta}{1-\sin(2\theta+\varphi)}$$

and the normal force per side F_n:

$$F_n=\frac{2\sigma_t d\sin(\theta+\varphi)\sin\theta}{1-\sin(2\theta+\varphi)}$$

The horizontal component of R_t is: $R_{th}=R_t\cos\left[\frac{\pi}{2}-(2\theta+\varphi)\right]=R_t\sin(2\theta+\varphi)$

The vertical component of R_t is: $R_{tv}=R_t\sin\left[\frac{\pi}{2}-(2\theta+\varphi)\right]=R_t\sin(2\theta+\varphi)$

The horizontal component of R_t is: $R_{wh}=R_w\cos\left[\frac{\pi}{2}-\varphi\right]=R_w\sin\varphi$

The vertical component of R_t is: $R_{wv}=R_w\sin\left[\frac{\pi}{2}-\varphi\right]=R_w\cos\varphi$

Evans also discussed teeth with a wear flat with the forces working on shown in Figure 31

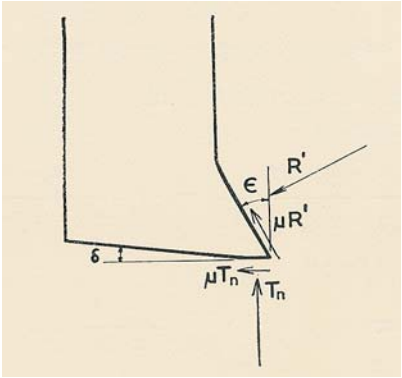

Figure 31

T_n is the normal force acting on the wear flat and μ the coefficient of friction between the rock and steel. F_c is the cutting force and F_n the normal force on the wedge. Hence:

$$F_c = R'\cos\varepsilon + \mu R'\sin\varepsilon + \mu T_n$$
$$F_n = \mu R'\cos\varepsilon - R'\sin\varepsilon + T_n$$

Assuming that μT_n is a small component of F_c, where as not a negligible of F_n, so the equaitions can be simplified to:

$$F_c = \frac{R'\cos(\varphi-\varepsilon)}{\cos\varphi}$$
$$F_n = \frac{R'\sin(\varphi-\varepsilon)}{\cos\varphi} + T_n$$
$$F_n = F_c\tan(\varphi-\varepsilon) + T_n$$

This results finally in:

$$F_c = \frac{2\sigma_t d\sin(\theta+\varphi)}{1-\sin(\theta+\varphi)} \text{ or } F_c = \frac{2\sigma_t d\sin\left\{\frac{1}{2}\left(\frac{\pi}{2}-\varepsilon\right)+\varphi\right\}}{1-\sin\left\{\frac{1}{2}\left(\frac{\pi}{2}-\varepsilon\right)+\varphi\right\}}$$

Sa that:

$$F_n = \frac{2\sigma_t d\sin\left\{\frac{1}{2}\left(\frac{\pi}{2}-\varepsilon\right)+\varphi\right\}}{1-\sin\left\{\frac{1}{2}\left(\frac{\pi}{2}-\varepsilon\right)+\varphi\right\}}\tan(\varphi-\varepsilon) + T_n$$

Resume

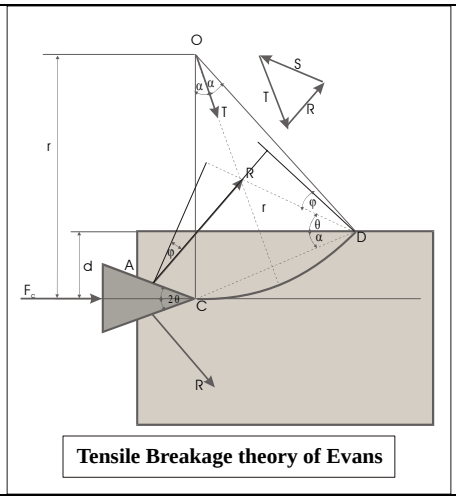

Tensile Breakage theory of Evans

$$F_c = \frac{2d\sigma_t \sin(\theta)}{1-\sin(\theta)}$$

$$F_n = \frac{2d\sigma_t \cos(\theta)}{1-\sin(\theta)}$$ (one side, $F_{n,total}$=0)

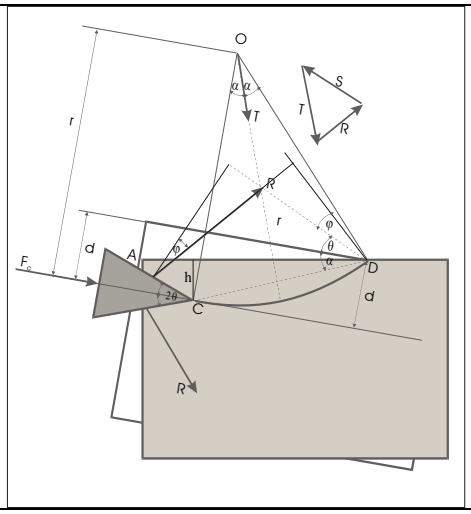

The horizontal component will be:

$$[F_c]_h = \frac{2h\sigma_t \sin\alpha}{\sin(\alpha-\varepsilon)} \cdot \frac{\sin(\theta+\varphi)}{1-\sin(\theta+\varphi)} \cos\varepsilon$$

and the vertical component:

$$[F_c]_v = \frac{2h\sigma_t \sin\alpha}{\sin(\alpha-\varepsilon)} \cdot \frac{\sin(\theta+\varphi)}{1-\sin(\theta+\varphi)} \sin\varepsilon$$

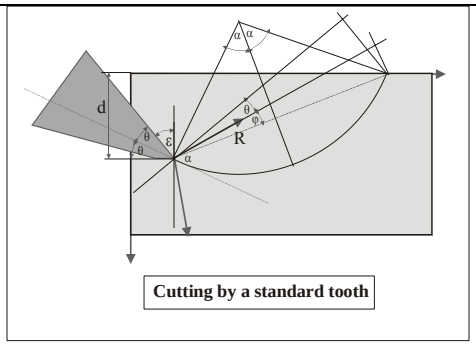

Cutting by a standard tooth

The cutting force F_c becomes:

$$F_c = \frac{2\sigma_t d \sin(\theta+\varphi)\cos\theta}{1-\sin(2\theta+\varphi)}$$

and the normal force per side F_n:

$$F_n = \frac{2\sigma_t d \sin(\theta+\varphi)\sin\theta}{1-\sin(2\theta+\varphi)}$$

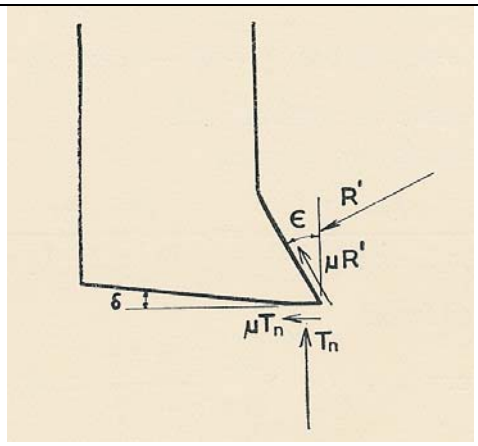

$$F_c = \frac{2\sigma_t d \sin\left\{\frac{1}{2}\left(\frac{\pi}{2}-\varepsilon\right)+\varphi\right\}}{1-\sin\left\{\frac{1}{2}\left(\frac{\pi}{2}-\varepsilon\right)+\varphi\right\}}$$

$$F_n = \frac{2\sigma_t d \sin\left\{\frac{1}{2}\left(\frac{\pi}{2}-\varepsilon\right)+\varphi\right\}}{1-\sin\left\{\frac{1}{2}\left(\frac{\pi}{2}-\varepsilon\right)+\varphi\right\}} \tan\left(\varphi-\varepsilon\right)+T_n$$

II. Model of Merchant

This model is original developed for cutting elastic-plastic metals and assumes failure to occur in shear. The depth of cut is small compared with the width of the cutting tool, so a condition of plane strain can be assumed.
The model is semi empirical. Merchant assumes that shear takes place over a line from the tip of the tool to the surface. However this model can be used too when plastic yield occurs only this line. In that case it is assumed that γ is small or zero. Experiments have shown that this theory is applicable for some kinds of coal and wet chalk.

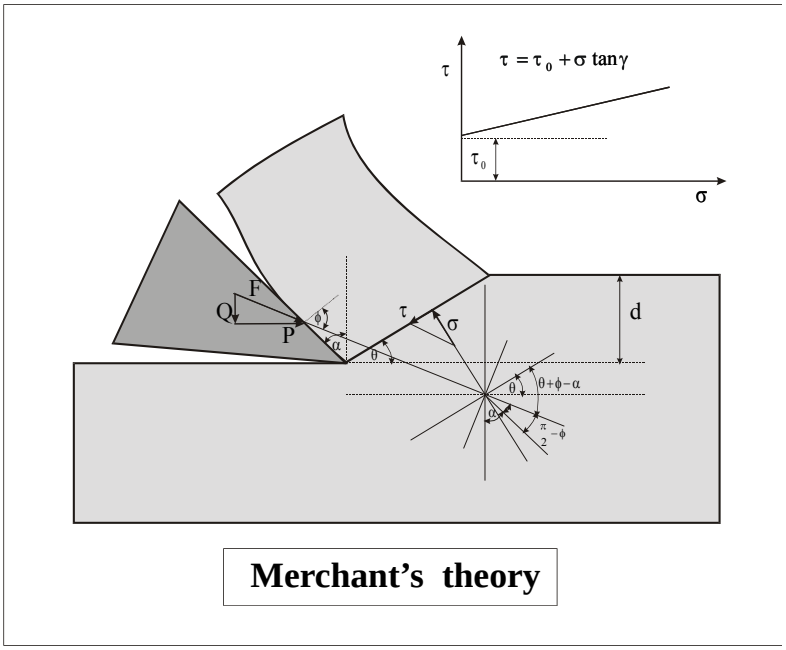

Figure 32

The model assumes a cohesion τ_0 and no adhesion and is therefore a particular situation of the theory of Dr.ir S.A. Miedema.

Equilibrium of forces gives:

$$\sigma = \frac{\sin\theta}{d} F \sin(\theta + \phi - \alpha)$$

and

$$\tau = \frac{\sin\theta}{d} F \cos(\theta + \phi - \alpha)$$

At the moment of failure:

$$\tau = \tau_0 + \sigma \tan\gamma$$

θ = angle of failure plane
ϕ = angle of total force with the normal
γ =angle of internal friction of the rock

Hence:

$$\tau = \tau_0 + \sigma \tan\gamma = \tau_0 + \frac{\sin\theta}{d} F \sin(\theta + \phi - \alpha) \tan\gamma = \frac{\sin\theta}{d} F \cos(\theta + \phi - \alpha)$$

or

$$\tau_0 \frac{d}{\sin\theta} = F \left[\frac{\cos(\theta + \phi - \alpha)\cos\gamma - \sin(\theta + \phi - \alpha)\sin\gamma}{\cos\gamma} \right] = F \frac{\cos(\theta + \phi - \alpha + \gamma)}{\cos\gamma}$$

It is assumed the angle θ can be determined by minimising the force F: so $\frac{dF}{d\theta} = 0$.

This results in

$$\frac{dF}{d\theta} = \frac{d}{d\theta}\left\{\frac{d}{\sin\theta}\frac{\tau_0\cos\gamma}{\cos(\theta+\phi-\alpha+\gamma)}\right\}$$

$$\frac{dF}{d\theta} = d\tau_0\cos\gamma\frac{\cos\theta\cos(\theta+\phi-\alpha+\gamma)-\sin\theta\sin(\theta+\phi-\alpha+\gamma)}{\sin^2\theta\left[\cos(\theta+\phi-\alpha+\gamma)\right]^2} = d\tau_0\cos\gamma\frac{\cos(2\theta+\phi-\alpha+\gamma)}{\sin^2\theta\left[\cos(\theta+\phi-\alpha+\gamma)\right]^2}$$

$\frac{dF}{d\theta} = 0$ for: $\cos(2\theta+\phi-\alpha+\gamma) = 0$

$$2\theta+\phi-\alpha+\gamma = \frac{\pi}{2} \Rightarrow \theta = \frac{\pi}{4}-\frac{1}{2}(\gamma+\phi-\alpha)$$

The force per unit of width is:

$$F = \frac{d}{\sin\left(\frac{\pi}{4}-\frac{1}{2}(\gamma+\phi-\alpha)\right)}\cdot\frac{\tau_0\cos\gamma}{\cos\left(\frac{\pi}{4}+\frac{1}{2}(\gamma+\phi-\alpha)\right)}$$

Further more

$$\sin\left(\frac{\pi}{4}-\frac{1}{2}(\gamma+\phi-\alpha)\right) = \sin\frac{\pi}{4}\cos\left\{\frac{1}{2}(\gamma+\phi-\alpha)\right\}-\cos\frac{\pi}{4}\sin\left\{\frac{1}{2}(\gamma+\phi-\alpha)\right\}$$
$$= \frac{1}{2}\sqrt{2}\left[\cos\left\{\frac{1}{2}(\gamma+\phi-\alpha)\right\}-\sin\left\{\frac{1}{2}(\gamma+\phi-\alpha)\right\}\right]$$

and
:

$$\cos\left(\frac{\pi}{4}-\frac{1}{2}(\gamma+\phi-\alpha)\right) = \cos\frac{\pi}{4}\cos\left\{\frac{1}{2}(\gamma+\phi-\alpha)\right\}-\sin\frac{\pi}{4}\sin\left\{\frac{1}{2}(\gamma+\phi-\alpha)\right\}$$
$$= \frac{1}{2}\sqrt{2}\left[\cos\left\{\frac{1}{2}(\gamma+\phi-\alpha)\right\}-\sin\left\{\frac{1}{2}(\gamma+\phi-\alpha)\right\}\right]$$

Hence:

$$F = \frac{2\cdot d\tau_0\cos\gamma}{\left[\cos\left\{\frac{1}{2}(\gamma+\phi-\alpha)\right\}-\sin\left\{\frac{1}{2}(\gamma+\phi-\alpha)\right\}\right]^2} = \frac{2\cdot d\tau_0\cos\gamma}{1-\sin(\gamma+\phi-\alpha)}$$

The horizontal cutting force is:

$$P = F_c = \frac{2\cdot d\tau_0\cos\gamma\cos(\phi-\alpha)}{1-\sin(\gamma+\phi-\alpha)}$$

en normal force:

$$Q = F_n = \frac{2\cdot d\tau_0\cos\gamma\sin(\phi-\alpha)}{1-\sin(\gamma+\phi-\alpha)}$$

The ratio between these forces is: $\frac{P}{Q} = \cot(\phi - \alpha)$

Because ϕ is unknown too, Merchant solved the problem by measuring ϕ from tests

The relation $\theta = \frac{\pi}{4} - \frac{1}{2}(\gamma + \phi - \alpha)$ determines if the failure is on shear or on tensile

The normal pressure is $\sigma = \frac{\sin\theta}{d} F \sin(\theta + \phi - \alpha)$ substituting $\theta = \frac{\pi}{4} - \frac{1}{2}(\gamma + \phi - \alpha)$ gives

$$\sigma = \frac{F}{d}\sin\left[\frac{\pi}{4} - \frac{1}{2}(\gamma + \phi - \alpha)\right]\sin\left[\frac{\pi}{4} - \frac{1}{2}(\gamma - \phi + \alpha)\right]$$

Because $F = \frac{2 \cdot d\tau_0 \cos\gamma}{\left[1 - \sin(\gamma + \phi - \alpha)\right]} \geq 0$ tensile stress ($\sigma<0$) can occur only when:

$\sin\left[\frac{\pi}{4} - \frac{1}{2}\gamma + \frac{1}{2}(\phi - \alpha)\right]\sin\left[\frac{\pi}{4} - \frac{1}{2}\gamma - \frac{1}{2}(\phi - \alpha)\right] < 0$,

or

$\left\{-\cos\left(\frac{\pi}{2} - \gamma\right) + \cos(\phi + \alpha)\right\} < 0$ or $\cos(\phi + \alpha) < \cos\left(\frac{\pi}{2} - \gamma\right)$

So $\alpha < \frac{\pi}{2} - \gamma - \phi \quad 0 < \frac{\pi}{4} - \frac{1}{2}(\gamma + \phi + \alpha)$ or

So tensile failure occurs ($\sigma<0$) if $(\gamma + \phi + \alpha) < \frac{\pi}{2}$ or as $\alpha < \frac{\pi}{2} - (\gamma + \phi)$

Example

Given

- For brittle failure use is made of the envelope according Hoek & Brown.
- The rock is a limestone with a ductility number m=4 and the transition between brittle and ductile is determined by the equation of Mogi $\sigma_1 = 4.2\sigma_3$
- Rake angle α=30°, friction angle between tool and rock ϕ=72°
- Cutting depth d=0.1 m

Solving

- Determine the cross point between the envelope of Hoek & Brown with equation of Mogi, results in σ/q_u=1.144 en τ/q_u=0.843
- Determine Mohr circle for that point. Centre at σ/q_u=1.466 and radius R/q_u=0.902
- Determine the slope of the envelope tan(γ)=0.3817
- Determine τ_0 (τ_0/q_u=0.406)
- Calculate the forces F, P en Q and the stresses σ en τ with the formula of Merchant. Results: F/q_u=0.691, P/q_u=0.513, Q/q_u=0.462, σ/q_u=1.335 en τ/q_u=0.9156

For small values of ϕ the rock fails brittle. A Mogi equation with a larger tangent results in a plastic cutting process for small values of ϕ. With high ϕ-values a wear flat can be simulated.

For $\sigma_1=6.5\sigma_3$ and $\phi = \frac{\pi}{3}$ gives the following Figure 31

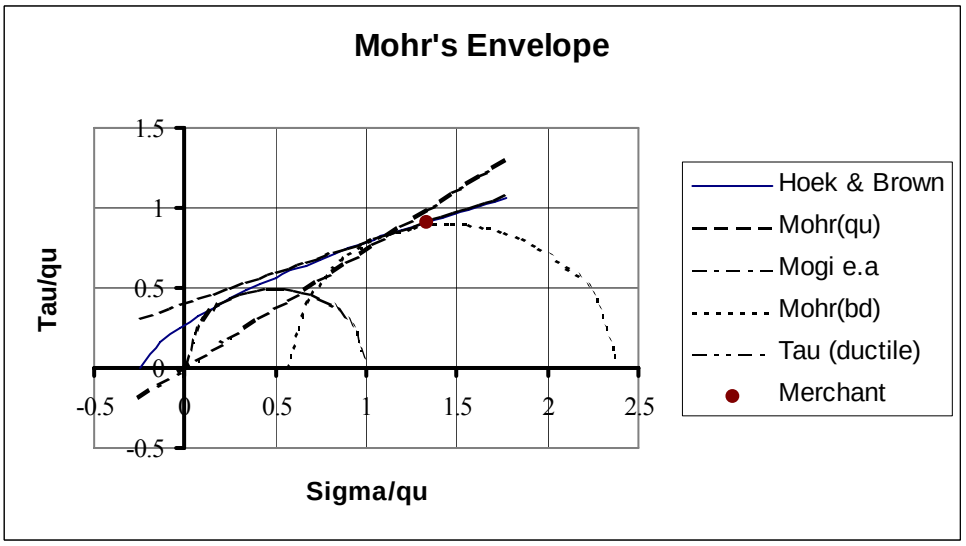

Figure 33

Model van Nishumatsu

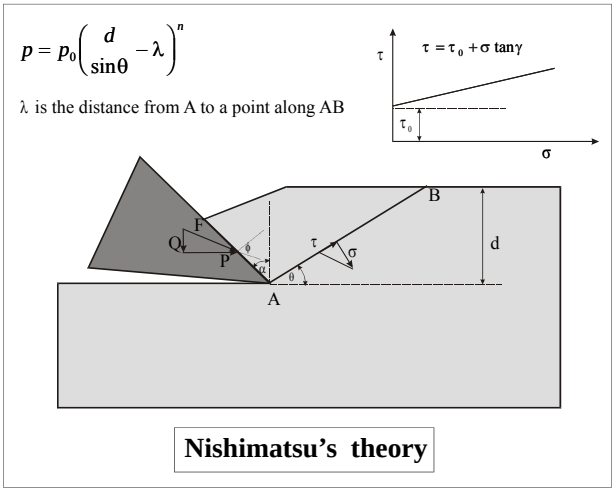

Figure 34

Nishimatsu presented a theory for the cutting of rock in which he assumes that the resulting stress p acting the failure line AB is proportional to the nth power of the distance from surface point B and is constant in magnitude and direction. So:

$$p = p_0\left(\frac{d}{\sin\theta} - \lambda\right)^n$$

The exponent n is called the stress distribution factor

Nishumatsu made the following assumptions:

- The rock cutting is brittle, without any accompanying plastic deformation (no ductile crushing zone)
- The cutting process is under plain stress condition
- The failure is according a linear Mohr envelope
- Te cutting speed has no effect on the processes.

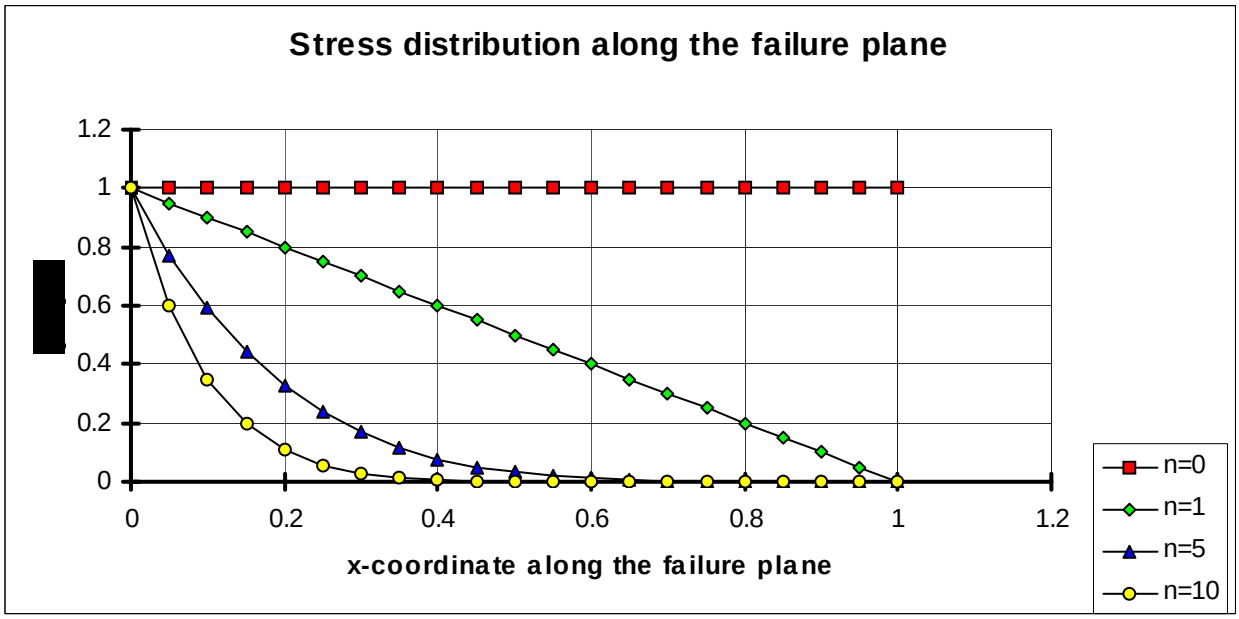

Figure 35

The integral of the resulting stress have to be in equilibrium with the force F.

$$F = p_0 \int_0^{\frac{d}{\sin\theta}} \left(\frac{d}{\sin\theta} - \lambda \right)^n d\lambda$$

Or

$$F = \frac{p_0}{(n+1)} \left(\frac{d}{\sin\theta} - \lambda \right)^{n+1} \quad of \quad p_0 = (n+1) \left(\frac{d}{\sin\theta} - \lambda \right)^{-(n+1)} F$$

Substituting this in equation:

$$p = p_0 \left(\frac{d}{\sin\theta} - \lambda \right)^n$$

results in

$$p = (n+1) \left(\frac{d}{\sin\theta} - \lambda \right) F$$

The maximum stresses σ and τ occurs for λ=0 and are:

$$\sigma = (n+1) \left(\frac{d}{\sin\theta} - \lambda \right) F \sin(\theta + \phi - \alpha)$$

$$\tau = (n+1) \left(\frac{d}{\sin\theta} - \lambda \right) F \cos(\theta + \phi - \alpha)$$

The general solution is:

$$F = \frac{2}{n+1} \cdot \frac{2 \cdot d\tau_0 \cos\gamma}{1 - \sin(\gamma + \phi - \alpha)}$$

$$P = F_c = \frac{2}{n+1} \frac{\cdot d\tau_0 \cos\gamma \cos(\phi - \alpha)}{1 - \sin(\gamma + \phi - \alpha)}$$

$$Q = F_n = \frac{2}{n+1} \frac{\cdot d\tau_0 \cos\gamma \sin(\phi - \alpha)}{1 - \sin(\gamma + \phi - \alpha)}$$

For n=0 this results in Merchant equation.

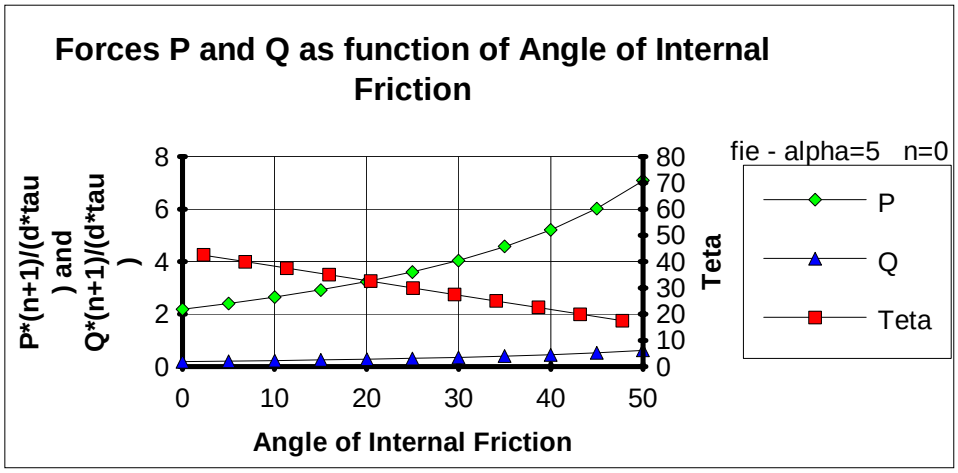

Figure 36

Influence of rake angle on the coefficient n

From tests it appeared that in a type of rock the value of n depends on the rake angle. (Figure 37) It should be mentioned that for this particular case n is about 1 for a small rake angle (large cutting angle). In that case tensile failure may give way to a process of shear failure, which is observed by other researches as well.

For rake angle large than 10 degrees n is more or less constant with a value of n=0.5

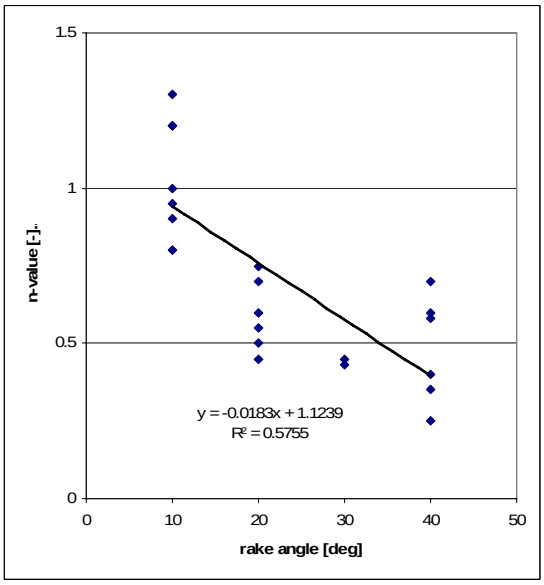

Figure 37

Specific energy of sharp and blunt cutting tools

Summarising the cutting force per unit width of the fore mentioned cutting theories are:

Table 6

Evans	$F_c = \frac{2d\sigma_t \sin(\theta+\phi)}{1-\sin(\theta+\phi)}$
Merchant	$F_c = \frac{2 \cdot d\tau_0 \cos\gamma \cos(\phi-\alpha)}{1-\sin(\gamma+\phi-\alpha)}$
Nishumatsu	$F_c = \frac{2}{n+1} \frac{\cdot d\tau_0 \cos\gamma \cos(\phi-\alpha)}{1-\sin(\gamma+\phi-\alpha)}$

The specific energy *SPE* is the energy required to cut 1 m^3 rock, which is equal to the power to cut 1 m^3/sec.
The power per unit width $P = F_c \cdot v_c$ with v_c the speed of the cutting tool. The production per unit width is $q = d \cdot v_c$ so $SPE = \frac{F_c \cdot v_c}{d \cdot v_c} = \frac{F_c}{d}$, which is according the fore mentioned theories

Table 7

Evans	$SPE = \frac{2\sigma_t \sin(\theta+\phi)}{1-\sin(\theta+\phi)}$
Merchant	$SPE = \frac{2\cos\gamma \cos(\phi-\alpha)}{1-\sin(\gamma+\phi-\alpha)}$
Nishumatsu	$SPE = \frac{2}{n+1} \frac{\tau_0 \cos\gamma \cos(\phi-\alpha)}{1-\sin(\gamma+\phi-\alpha)}$

These theories are applicable for intact rock and sharp cutting tools.

From different experiments it appears that cutting force and the normal force can be written as:

$$P = a_c + b_c d$$
$$Q = a_n + b_n d$$

According Nishimatsu first terms (a_c en a_n) are caused by the existence of the crushed zone. The terms b_c en b_n correspond with the equation of P en Q mention in the simple models.
Other investigators (Adachi, 1996) state that the terms a_c en a_n are a result of the weir of the cutting tool and state for sharp tools $a_c = a_n = 0$
Both effects are not contradictory to each other.

As stated earlier: $Q = P\tan(\phi-\alpha) = \zeta P$ met $\zeta = \tan(\phi-\alpha)$

If the area cut is equal to $A = wd$, then for sharp tools the following results are valid:

$$P_s = b_c wd$$
$$Q_s = b_n wd = \zeta \cdot b_c wd$$

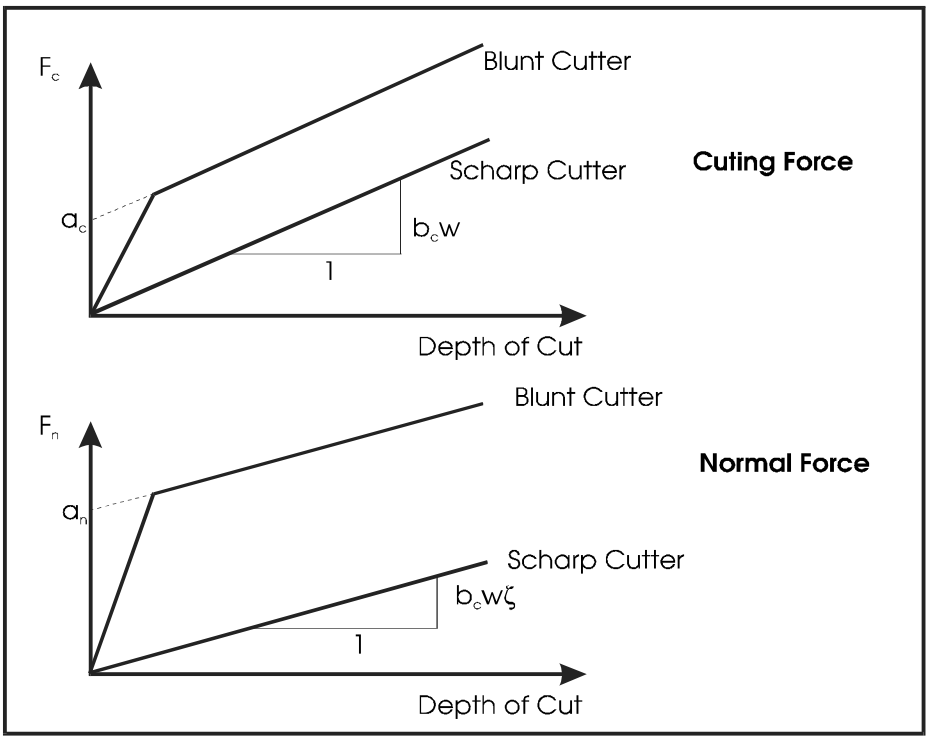

Figure 38

The specific energy of the cutting force and normal force for sharp tools become:

$$SPE_c^s = \frac{Pv}{wdv} = \frac{P}{wd} = \frac{b_c wd}{wd} = b_c$$
$$SPE_n^s = \frac{Qv}{wdv} = \frac{Q}{wd} = \frac{\zeta \cdot b_c wd}{wd} = \zeta \cdot b_c$$
$$\text{with } \frac{b_n}{b_c} = \zeta$$

Or: $\frac{SPE_n^s}{SPE_c^s} = \frac{Q}{P} = \zeta$ is constant. This equation can be written as:

$$SPE_c^s = \frac{1}{\zeta} SPE_n^s$$

Adachi (1996) reports that, according that research from researcher in the field of cutting tools for the oil-industry, there is a clear experimental evidence that the value ζ depends on the type of cutting tool and is independent of the rock material.

For blunt tools this becomes:

$$SPE_c^b = \frac{P}{wd} = \frac{a_c + b_c wd}{wd} = \frac{a_c}{wd} + b_c$$
$$SPE_n^b = \frac{Q}{wd} = \frac{a_n + b_n wd}{wd} = \frac{a_n}{wd} + b_n = \frac{a_n}{wd} + \zeta \cdot b_c$$

In which the factors $\frac{a_c}{wd}$ en $\frac{a_n}{wd}$ do have the dimension of specific energy [N/m²]
The second equation can be written as:

$$SPE_n^b = \frac{a_n}{wd} + \zeta \cdot \left(SPE_c^b - \frac{a_c}{wd} \right)$$

or

$$SPE_c^b = \frac{a_c}{wd} - \frac{1}{\zeta}\frac{a_n}{wd} + \frac{1}{\zeta} SPE_n^b$$

resulting in

$$SPE_c^b = SPE_0 + \frac{1}{\zeta} SPE_n^b$$

with

The ratio between the forces P en Q is:

$$\frac{SPE_n^b}{SPE_c^b} = \frac{Q}{P} = \zeta \frac{SPE_c^b - SPE_0}{SPE_c^b} = \zeta \left(1 - \frac{SPE_0}{SPE_c^b} \right)$$

which is not constant, besides $\left| \frac{SPE_0}{SPE_c^b} \right| =<< 1$

$$\frac{SPE_0}{SPE_c^b} = \frac{\frac{a_c}{wd} - \frac{1}{\zeta}\frac{a_n}{wd}}{\frac{a_c}{wd} + b_c} = \frac{1 - \frac{1}{\zeta}\frac{a_n}{a_c}}{1 + \frac{b_c wd}{a_c}}$$

When a_c en a_n are determined by friction $\frac{a_c}{a_n} = \mu = 0.6$. Furthermore for sharp tools $\zeta<0.66$ and is $\frac{b_c wd}{a_c} > 1$; *not* fulfilling the condition $\left| \frac{SPE_0}{SPE_c^b} \right| =<< 1$

Practical applications of the cutting theories

During cutting, a single cutting tool experiences a force F, having three orthogonal components:

- in the direction parallel to the soil surface, the Cutting Force C
- perpendicular to the surface the Normal Force N
- a sideways or Lateral Force L (Fig. 34)

The Lateral Forcer L is mainly caused by the interaction of neighbouring cuts. This force may be
neglected for cylindrical cutter heads with staggered teeth on the cutter head blades

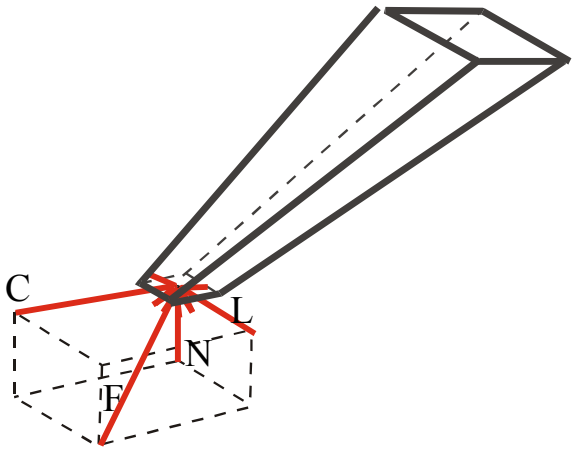

Figure 39

Cutter heads, however, have very seldom a cylindrical shape but rather have profiles as shown in Figure 37
This profile is determined by a plane through the surface of revolution formed by the tooth points. The cutter teeth are normally positioned in such a way that the projection of it's centre line is normal to the profile. This results in a break out pattern as shown in figure 39.
The Normal Force N has two orthogonal components Ncosκ and Nsinκ, respectively perpendicular and parallel with the cutter shaft.

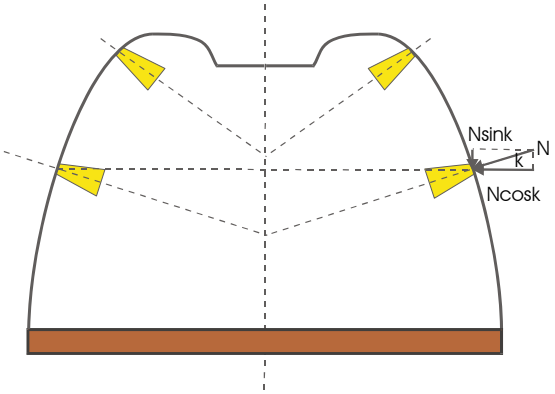

Figure 40

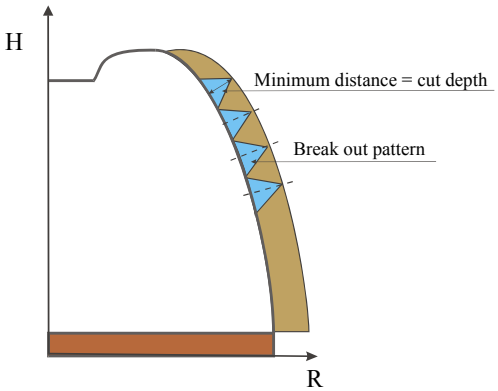

In a plane perpendicular to the axe of rotation, a tooth on a cutter head experiences a force F having
two components: in the direction parallel to the soil surface, the Cutting Force C, and perpendicular to the surface, the Normal Force, Ncosκ (Figure 37). In the direction perpendicular this plane the tooth is subjected to the force Nsinκ

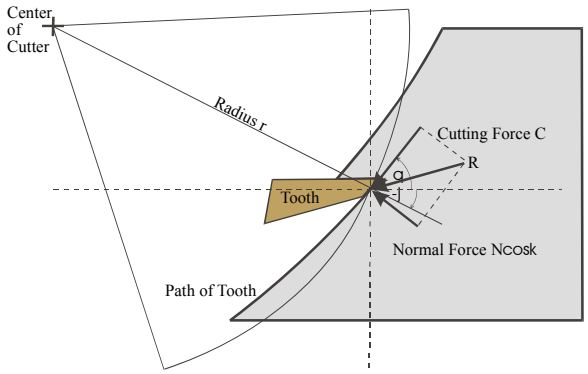

Figure 41

Both forces in can be decomposed either in (Fig. 36):

- Horizontal Force H and a Vertical Force V, or in
- cutter head related co-ordinates; tangential Force T and the radial force R
-

From Figure 38 follows:

$$T = C\sin(\theta-\varphi) - N\cos\kappa\cos(\theta-\varphi)$$

$$R = C\cos(\theta-\varphi) - N\cos\kappa\sin(\theta-\varphi)$$

$$H = C\cos\theta - N\cos\kappa\sin\theta$$

$$V = C\sin\theta - N\cos\kappa\cos\theta$$

It was already stated that the axial force is

$$A = N\sin\kappa$$

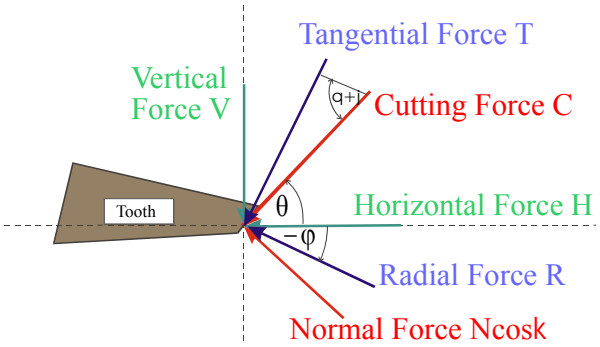

Figure 42

Using the theory as discussed earlier for a single cutting tools the Cutting Force C and the N Normal N are proportional with the depth of cut to: $C = a_c + b_c d$ and $N = a_n + b_n d$.

Substitution of the equation for the Normal Force in the one for the Cutting Force results in:

$C = a_c - \frac{b_c}{b_n}a_n + \frac{b_c}{b_n}N$ which can be written as $C = C_0 + \frac{b_c}{b_n}N$

When the last expression is substituted in the equation for T, R, H and V results in:

$$T = C_0\sin(\theta-\varphi) + N\left[\frac{b_c}{b_n}\sin(\theta-\varphi) - \cos\kappa\cos(\theta-\varphi)\right]$$

$$R = C_0\cos(\theta-\varphi) + N\left[\frac{b_c}{b_n}\cos(\theta-\varphi) + \cos\kappa\sin(\theta-\varphi)\right]$$

$$H = C_0\cos\theta + N\left[\frac{b_c}{b_n}\cos\theta + \cos\kappa\sin\theta\right]$$

$$V = C_0\sin\theta + N\left[\frac{b_c}{b_n}\sin\theta - \cos\kappa\cos\theta\right]$$

All forces are a function of the parameters C_0, N, θ, φ, and κ of which θ, φ, and κ are determined by the tooth position during cutting.

The angles θ and φ depend on the cutter head speed ω and the swing speed v_s according to:

$x_c = r \cdot (m\varphi + \cos\varphi)$ and $y_c = r \cdot (1 + \sin\varphi)$

x_c=x-coordinate cutting tool point in m.
y_c= y-coordinate cutting tool point in m
r=radius of cutting tool point to cutting axes in m
while

$m = \frac{v_s}{\omega r}$ *and* $\varphi = \omega t$ with t is the time in seconds

By differentiating of x_c and y_c gives

$\frac{dy_c}{dx_c} = \frac{dy_c}{d\varphi}\frac{d\varphi}{dx_c} = \frac{\cos\varphi}{m - \sin\varphi} = \tan\theta$ and according to *Figure 40*

Or

$\varphi = \theta - \arccos(m\sin\theta)$

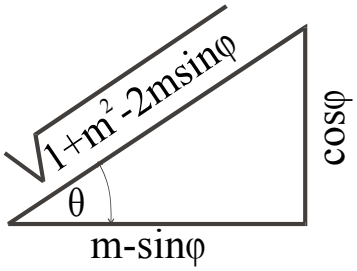

Figure 43

According to Figure 41 the depth of cut

$d = \frac{v_s}{\omega p}\sin\theta\cos\kappa$

with:
v_s= swing speed of the cutter in m/s
ω=the angular speed of the cutter in radians/s
p=the number of blades on the cutter
κ= profile angle in radians

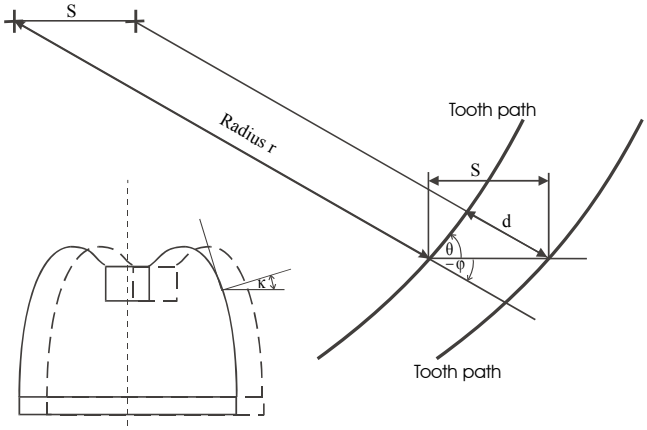

Figure 44

Substituting the equation for the depth din the equation for the Normal Force $N = a_n + b_n d$ results in $N = a_n + b_n \frac{v_s}{\omega p}\sin\theta\cos\kappa$

If the coefficients C_0, a_c, a_n, b_c and b_n are known all forces can be calculated as function of the position of the cutting tool point

Literature

- P. N.W Verhoef, Wear of Rock Cutting Tools, Balkema, Rotterdam/Brookfield, 1997.
- C. Fairhurst, On the Validity of the Brazilian Test for Brittle Materials, Int J.Rock Mech. Mining Sci. Vol.1 pp. 535-546 Pergamon Press 1964.
- E. Hoek & E.T. Brown, Underground excavation in rock, The Institute of Mining and Metallury, London, 1980.
- E. Hoek, P.K. Kaiser & W.F. Brawden, 1995 Support of underground excavations in hard rock, Balkema, Rotterdam.
- W.G.M. van Kesteren, Numerical simulations of crack bifurcation in the chip forming process in rock. In G. Baker & B.L. Karihaloo *Fracture of brittle dusordered material: concrete, rock and ceramics;* paper 33 E&FN Spon, London
- A.A. Evans, I & Pomeroy, C.D. (1966) *The strenght, fracture and workability of coal*, Pergamon Press.
- Comprehensive Rock Engeering, Volume 1, John A. Hudson, Pergamon Press,1993
- Nishimatsu, Y. (1972) "The mechanics of rock cutting." *Int. J. Mining Science": 9, 262-270*
.
- Roxborough, F.F. (1973). "Cutting rocks with picks." *The mining engineer:* June 1973
- Roxborough, F.F. (1973). "A laboratory investigation into the application of picks for mechanised tunnel boring in the lower chalk." *The mining engineer:* Oktober 1973
- Adachi, J.I. (1996), “frictional contact in rock cutting with blunt tools”, master degree thesis, University of Minnesota
- Pells, P.J.N. Uniaxial strength testing. In J.A. Hudson (ed.*) Comprehensive rock engineering, vol. 3, Rock testing and site characterization:* 67-85. Pergamon press, Oxford.
- Verhoef, Peter N.W. *Wear of rock cutting tools,* A.A, Balkema/Rotterdam/Brookfiels, 1997, ISDN 90 5410 434 1
- Vlasblom, W.J. Relation between Cutting, Sidewinch and Axial Forces for Cutter Suction dredgers, *15th World Dredging Congress, Las Vegas, Nevada, USA,* June 28-July 2, 1998, Volume 1